

CONODONT COLOR ALTERATION:
A POSSIBLE EXPLORATION TOOL FOR ORE DEPOSITS

by

Kevin H. Cook

Submitted in Partial Fulfillment
of the Requirements for the Degree of
Master of Science in Geology

New Mexico Institute of Mining and Technology
Socorro, New Mexico

January, 1986

ABSTRACT

The purpose of this thesis was to test hypotheses relating the alteration of conodont-color to thermal environments associated with the deposition of economic minerals. The Hansonburg Mississippi Valley-type deposit and Continental copper skarn deposit were studied to determine whether a relationship exists between the alteration of conodont-color and hydrothermal activity. The Central Tennessee Mississippi Valley-type deposit was studied to determine whether this relationship could be used as an exploration tool for blind ore deposits.

Carbonate rock, silica, and hydrothermally deposited minerals were collected at each deposit for measurement of conodont-color, size of silica-crystallites, and fluid inclusion temperatures. Conodonts were separated from host carbonate rocks and conodont color alteration indices (CAI) were determined using a set of field standards. Fluid inclusion and silica-crystallite geothermometry were used as independent checks of temperatures for these deposits.

In the Hansonburg mining district, conodont CAI increase from 1 to 3 toward the deposit, with 3 being closest to the mineralization. CAI of 1 represent background values, and CAI from 1.5 to 3 represent anomalous values. These anomalous values surround the deposits and extend up to 400 meters from known occurrences of mineralization.

CAI from 3 to 6 were measured in conodonts recovered from near the Continental mine. These CAI increase in value towards the Hanover-Fierro stock, which is genetically related to copper mineralization. These CAI surround the intrusive extending up to 5 kilometers from the pluton, suggesting that this area was extensively heated during the emplacement of the stock.

In the Central Tennessee mining district CAI from 1 to 2.5 were measured. CAI of 1 represent background values, and CAI of 1.5, 2, and 2.5 represent anomalous values. Anomalous CAI are regionally extensive and stratigraphically distributed, with 1.5 to 2 occurring low in the stratigraphic section and 2.5 occurring high in the stratigraphic section. The stratified nature of CAI in the Central Tennessee mining district suggests that the highest temperatures were located near the top of the hydrothermal system.

Published temperatures (Epstein et al., 1977) associated with anomalous CAI are in close agreement with fluid inclusion homogenization temperatures measured in hydrothermally deposited minerals. Temperatures determined from the size of silica-crystallites do not correlate well with fluid inclusion homogenization temperatures or the published temperatures associated with anomalous CAI.

I contend that the anomalous CAI observed near mineral deposits in this thesis indicate that alteration of conodont color is affected by hydrothermal activity associated with

the emplacement of mineral deposits. Therefore, this technique can be used to delineate regions exposed to hydrothermal activity.

ACKNOWLEDGMENTS

I wish to thank all of those involved with this project, especially the members of my thesis committee: Dr. David B. Johnson and Dr. David I. Norman (coadvisors), Dr. Jacques Renault, Dr. Jay Gregg, and Dr. Andrew Campbell. All of the above lent their expertise to portions of this study.

I would like to acknowledge the generous financial support provided by St. Joe Minerals Corporation. The State Mining and Mineral Resources Research Institute at the New Mexico Institute of Mining and Technology also provided much needed financial assistance.

I also would like to thank the companies and people at the respective mines for permission to work at their properties and the valuable advice they provided: Dean Duke and Sam Jones at the Hansonburg mining district, Owen Hart of Sharon Steel Corporation at the Continental mine, and Jay Gregg and Bruce Ahler of St. Joe Minerals Corporation for providing core from the Central Tennessee mining district.

Thanks also to the many friends and colleagues I have had the good fortune to meet at New Mexico Tech. The many discussions among fellow students has aided in my development as a geologist and person.

Finally I wish to express my greatest thanks to Sylveen Robinson, my wife to be, and to my parents for their encouragement and moral support throughout this endeavor. Thank you for all your support.

TABLE OF CONTENTS

Abstract.....	i
Acknowledgments.....	iv
Table of Contents.....	v
List of Figures.....	vii
List of Tables.....	ix
Introduction.....	1
Purpose of Investigation.....	1
Background.....	1
Assumptions.....	4
Geologic Settings.....	5
Hansonburg Mining District.....	5
Continental Mine.....	11
Methods of Investigation.....	16
Sampling.....	16
Hansonburg Mining District.....	16
Continental Mine-Central Mining District.....	18
Sample Preparation.....	19
Analysis.....	20
Geothermometry.....	21
Results.....	22
Hansonburg Mining District.....	22
Recovery.....	22
Conodont CAI.....	23
Fluid Inclusion Study.....	31
Material Studied.....	31
Temperatures of Homogenization.....	32
Silica Crystallite Size.....	32
Continental Mine.....	36
Recovery.....	36
Conodont CAI.....	36
Fluid Inclusion Study.....	39
Material Studied.....	39
Temperatures of Homogenization.....	42
Silica Crystallite Size.....	42
Confirmation of Assumptions.....	45
Interpretation.....	51
Hansonburg Mining District.....	51
Continental Mine.....	59
Applicability of Method.....	66

Central Tennessee Mining District.....	68
Introduction.....	68
Geologic Setting.....	68
Sampling.....	74
Results.....	75
Recovery.....	75
Conodont CAI.....	75
Fluid Inclusion Microthermometry.....	76
Material Studied.....	76
Temperature of Homogenization.....	79
Temperature of Melting.....	82
Silica Crystallite Size.....	82
Interpretation of Central Tennessee.....	84
Conclusions.....	92
Suggestions for Future Study.....	94
References.....	95
Appendix I Conodont Color Alteration Data.....	101
Part A Hansonburg Mining District.....	102
Part B Continental Mine.....	111
Part C Central Tennessee Mining District.....	115
Appendix II Fluid Inclusion Data.....	119
Appendix III Chert Crystallite Size Data.....	125

LIST OF FIGURES

FIGURE	DESCRIPTION	PAGE
Figure 1	Generalized geologic map of the Hansonburg mining district, showing major structures and sample locations.	6
Figure 2	Stratigraphic column of Pennsylvanian and lower Permian rock units in the vicinity of the Hansonburg mining district.	8
Figure 3	Generalized geologic map of the northern portions of the Santa Rita Quadrangle, showing major structures and sample locations.	12
Figure 4	Conodont CAI map of the Hansonburg mining district showing distribution of highest CAI in each sample.	24
Figure 5	Stratigraphic distribution of CAI in conodonts recovered from samples collected near the Mex-Tex and Royal Flush mines, Hansonburg mining district.	26
Figure 6	Lateral distribution of CAI in conodonts recovered from samples collected from the Council Springs Limestone and Burrego Formation near the Mex-Tex, Royal Flush-Mountain Canyon Mines, and at Hansonburg Hill.	28
Figure 7	Histogram of temperatures of homogenization for fluid inclusions in calcite sample HH1 and quartz sample MT1.	33
Figure 8	Conodont CAI map in the northern portion of the Santa Rita quadrangle.	37
Figure 9	Distribution of CAI in conodonts collected near the Hanover-Fierro stock.	40
Figure 10	Histogram of temperature of homogenization for inclusions in samples MP2, MP3, and MLV8 from the Continental mine.	43
Figure 11	Comparison of temperatures related to conodont CAI, fluid inclusion homogenization temperatures, and temperatures determined from the diameter of silica-crystallites.	46

Figure 12	Arrhenius plot of temperature versus time, showing predicted CAI associated with deposition of hydrothermal minerals in the Hansonburg mining district.	53
Figure 13	Conodont CAI contour map showing the extent of anomalous CAI in the Hansonburg mining district.	57
Figure 14	Arrhenius plot of temperature versus time showing predicted CAI associated with temperatures of skarn formation and mineral deposition near the Continental mine.	60
Figure 15	Conodont CAI contour map of the northern portion of the Santa Rita quadrangle showing extent of thermal anomaly around the Haover-Fierro stock.	63
Figure 16	General location and drill site location map of the Central Tennessee mining district.	69
Figure 17	Profile showing sample locations and distribution of mineralization in drill cores from the Central Tennessee mining district.	72
Figure 18	Lateral and stratigraphic distribution of conodont CAI relative to mineralization in the Central Tennessee mining district.	77
Figure 19	Range of temperature of homogenization and melting for fluid inclusions in sphalerite and fluorite from the Central Tennessee mining district.	80
Figure 20	Arrhenius plot of temperature versus time, showing predicted CAI associated with the deposition of hydrothermal minerals in the Central Tennessee mining district.	85
Figure 21	Conodont CAI contour profile showing proposed distribution of CAI in the Central Tennessee mining district.	89

LIST OF TABLES

TABLE	DESCRIPTION	PAGE
Table 1	Correlation of conodont CAI to temperatures.	3
Table 2	Temperatures calculated from the size of silica-crystallites for samples of nodular cherts and jasperoids collected in the Hansonburg mining district.	35
Table 3	Contingency table of conodont CAI versus size of conodonts recovered from the Hansonburg mining district and the northern portion of the Santa Rita quadrangle.	48
Table 4	Temperatures calculated from the size of silica-crystallites for samples of nodular chert in the Central Tennessee mining district.	83

INTRODUCTION

PURPOSE OF INVESTIGATION

The purpose of this study was to test two hypotheses relating the alteration of conodont-color to thermal environments associated with the deposition of economic minerals:

- 1). The alteration of conodont-color is affected by relatively short term thermal activity related to ore deposition.
- 2). Progressive changes in conodont-color can be used to locate an ore deposit by defining the thermal aureole around the deposit.

These hypotheses were tested at the Hansonburg mining district and the Continental mine, because these deposits are located on the surface, providing easy access to the deposits and excellent control of sampling. Conodonts recovered from carbonate samples of drill core from the Central Tennessee mining district were studied to determine whether this technique can be used as an exploration tool for blind ore deposits.

Background

Conodonts are microscopic, tooth-like hardparts of a group of marine organisms for which zoological affinities are not known. These organisms existed from Middle Cambrian through Triassic time. They occur worldwide in most marine sedimentary rock types and are most easily extracted from carbonate rocks. Conodonts are highly resistant to

physical, biological, and chemical destruction as a result of their small size and mineralogical composition.

Epstein et al. (1977) observed changes in conodont-color using controlled time-temperature-pressure experiments in wet and dry systems. Changes in color produced in the laboratory were compared to colors of conodonts recovered from field collections. From their study they concluded that:

- 1). The alteration of conodont-color is time and temperature dependent.
- 2). Changes in conodont-color are progressive and irreversible. Conodonts sequentially change in color from pale yellow (unaltered) to brown to black to gray to opaque white to crystal clear.
- 3). Changes in color from yellow to black is a result of a carbon-fixing process of interstitial organic matter, and color changes from black to crystal clear results from a carbon-loss process, release of water of crystallization, and recrystallization.
- 4). The alteration of color in conodonts is relatively independent of pressure.

From their work, Epstein et al. (1977) developed the concept of conodont color alteration indices (CAI), which correlate conodont-colors to specific range of temperatures. The range of CAI's is one to eight suggesting temperatures from less than 50°C to greater than 450°C (Table 1).

Conodont-color may be influenced by differences in the structural makeup among conodont types (Barnes et al., 1973), the size, shape, and maturity among conodont elements (Epstein et al., 1977), and host rock lithology (Epstein et al., 1977; Legall et al., 1981; Mayr et al., 1978).

Table 1
 Correlation of conodont CAI to temperatures (after Epstein et al., 1977). Processes responsible for color alteration are shown on the right side of the table.

CAI	TEMPERATURES (°C)	CONODONT-COLOR		
1	50-80	Pale Yellow	CARBON-FIXING	PROCESS RESPONSIBLE FOR COLOR ALTERATION
15	50-90	Very Pale Brown		
2	60-140	Brown to Dark Brown		
3	110-200	Very Dark Grayish Brown		
4	190-300	Brownish Black		
5	300-400	Black		
6	300-400	Gray	CARBON-LOSS	
7	400-450	Opaque White		
8	450+	Crystal Clear		

Conodont CAI have been used to determine temperatures resulting from long term burial (Bergstrom, 1980; Epstein et al., 1977; Gray, 1981; L. Harris et al., 1981; Legall et al., 1981; Nowlan et al., 1983; Perry et al., 1979; Perry et al., 1983; Spung and Groshong, 1981; Wardlaw and Harris, 1984). As a result, this technique has provided information in targeting favorable sites for oil and gas (Epstein et al., 1977; L. Harris et al., 1981; Mayr et al., 1978; Perry et al., 1983; Sando et al., 1981; Wardlaw and Collinson, 1978).

Conodonts with anomalously high CAI were recovered from mining districts in Utah, Nevada, and Arizona (Wardlaw and Collinson, 1978; Wardlaw and Harris, 1984). Other thermal alteration indicators, such as vitrinite reflectance, have been used to record thermal aureoles around ore deposits (Duba and Williams-Jones, 1983; Ilchick, 1984). These works suggest that the alteration of conodont-color might be affected by temperatures from hydrothermal activity.

Assumptions

The following assumptions were made before undertaking this study:

- 1). The relationship between conodont-color and temperature, proposed by Epstein et al. (1977), is correct.
- 2). The alteration of conodont-color has little dependence on size of a conodont.
- 3). Conodonts were not removed from their original sites of deposition by processes of reworking and stratigraphic leakage.

GEOLOGIC SETTINGS

Hansonburg Mining District

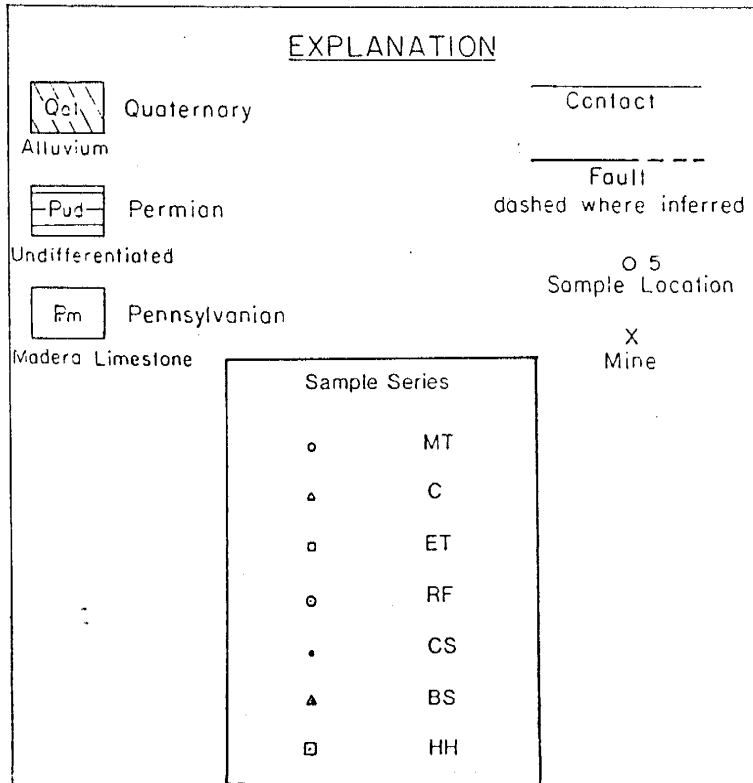
The Hansonburg mining district is located in the northern Oscura Mountains, eastern Socorro County, New Mexico (Fig. 1).

The Oscura Mountains form the eastern-most boundary of the Rio Grande Rift (Chapin, 1979). These mountains are characterized by a steep fault scarp to the west and gently dipping (<70) highlands to the east. The area consists principally of upper Pennsylvanian carbonate rocks, which unconformably overlie Precambrian granitic rocks and underlie Permian clastic rocks. Pennsylvanian rocks in the mining district were named the Madera Limestone by Wilpolt and Wanek (1951). Thompson (1942) divided the Pennsylvanian rocks near the district into eight distinct stratigraphic units (Fig. 2); the Bolander Group, Coane and Adobe Formations, Council Spring Limestone, Burrego, Story, Del Cuerto, and Moya Formations.

Economic minerals in the Hansonburg mining district consist of galena, barite, and fluorite. Hydrothermally deposited quartz, calcite, and siderite are also present. Minerals occupy open space fillings in podiform dissolution cavities. Mineralization within these cavities displays a banded texture, consisting of alternating layers of galena, barite, fluorite, and silicified limestone (jasperoid). These cavities are confined to the Council Spring Limestone

Figure 1

Generalized geologic map of the Hansonburg mining district, showing major structures and sample locations (after Putnam and Norman, 1983).



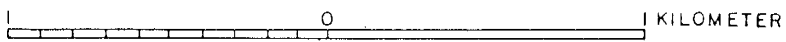
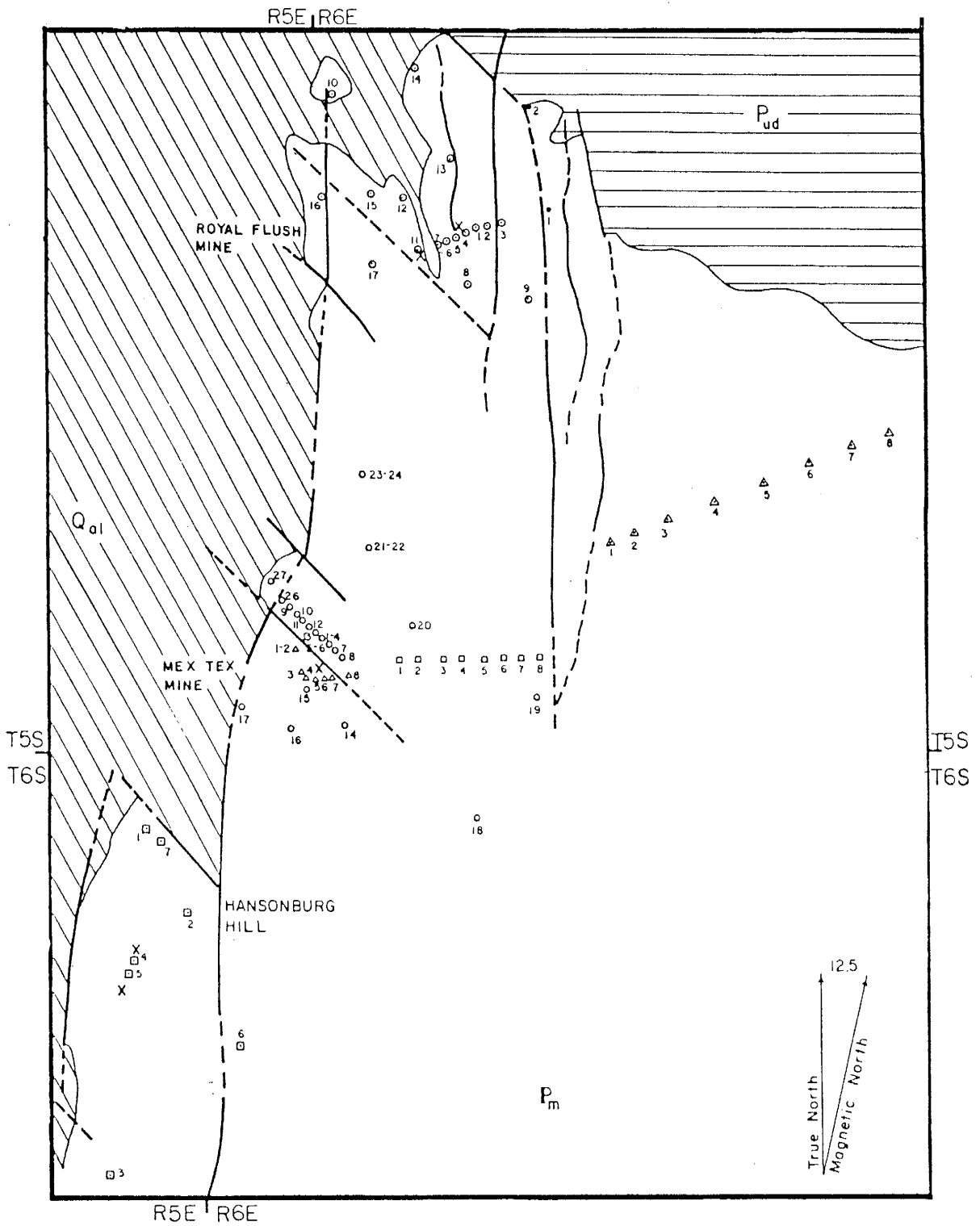


Figure 2

Stratigraphic column of Pennsylvanian and Lower Permian rock units in the vicinity of the Hansonburg mining district (after Kottowski, 1953).

PERIOD	FORMATION	THICKNESS (METERS)
PERMIAN	Bruton Formation	60
UPPER PENNSYLVANIAN	Moya Formation	15
	Del Cuerto Formation	25
	Story Formation	18
	Burrego Formation	16
	Council Spring Ls.	6
	Adobe Formation	14
	Coane Formation	23
	Bolander Group	37+

and lower Burrego Formation near minor northeast and northwest trending faults.

The geochemistry of deposits in the Hansonburg mining district have been studied by Roedder et al. (1968), Beane (1974), Allmendinger (1975), Ewing (1979), Putnam and Norman (1983), and Norman et al. (1985). Roedder et al. (1968) measured fluid inclusion homogenization temperatures and temperatures of melting in fluorite from the Hansonburg mining district. Temperatures of homogenization measured by Roedder and coworkers were between 140°C and 195°C, and temperatures of melting from -7.0°C to -13.0°C were measured, indicating salinities from 10 to 15 eq. wt. % NaCl. According to Roedder et al. (1968) temperatures of trapping were 18 degrees higher than temperatures of homogenization. Beane (1974) and Allmendinger (1975) proposed that the source of lead and sulfur in the deposit was from overlying Permian sedimentary rocks. Ewing (1979) suggested that the Precambrian granitic rocks supplied lead for the deposit. Putnam and Norman (1983) measured temperatures of homogenization from 125°C to 210°C and temperatures of melting from -6°C to -14°C in quartz and fluorite from the mining district. W. Ting (pers. comm., 1984) measured temperatures of homogenization and temperatures of melting in inclusions of calcite collected from limestones, which were collected within 6 meters of the present study's sample locations. Ting's measurements show

an increase in temperatures with proximity to the mineral deposit at the Royal Flush mine. Salinities determined by Ting are similar to salinities determined for fluid inclusions in fluorite and quartz by Roedder et al. (1968) and Putnam and Norman (1983). Norman et al. (1985) studied the composition of CO₂, CnHn, and N₂ gases in fluid inclusions from Hansonburg. Their study concluded that mineralization was emplaced under pressures of 150 to 200 bars and that the episode of mineral deposition occurred sometime between 26 and 7 million years ago in response to the cooling of hydrothermal fluids.

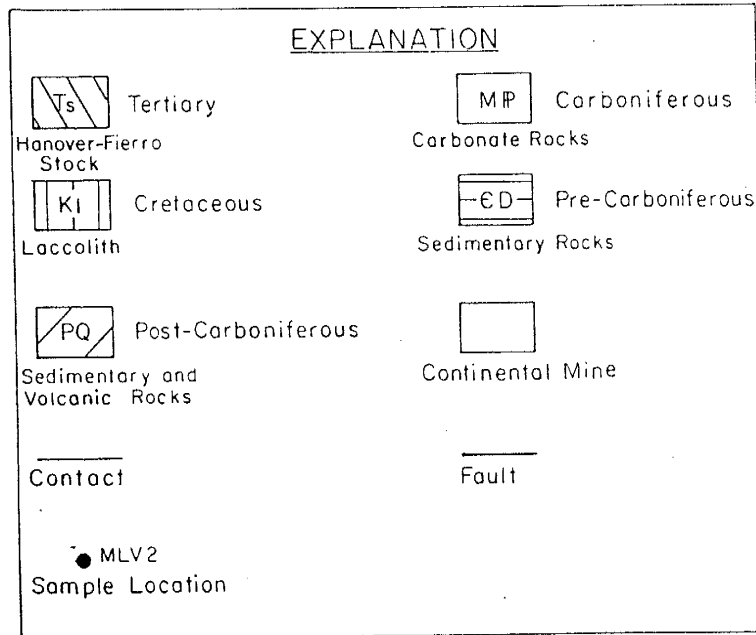
Continental Mine

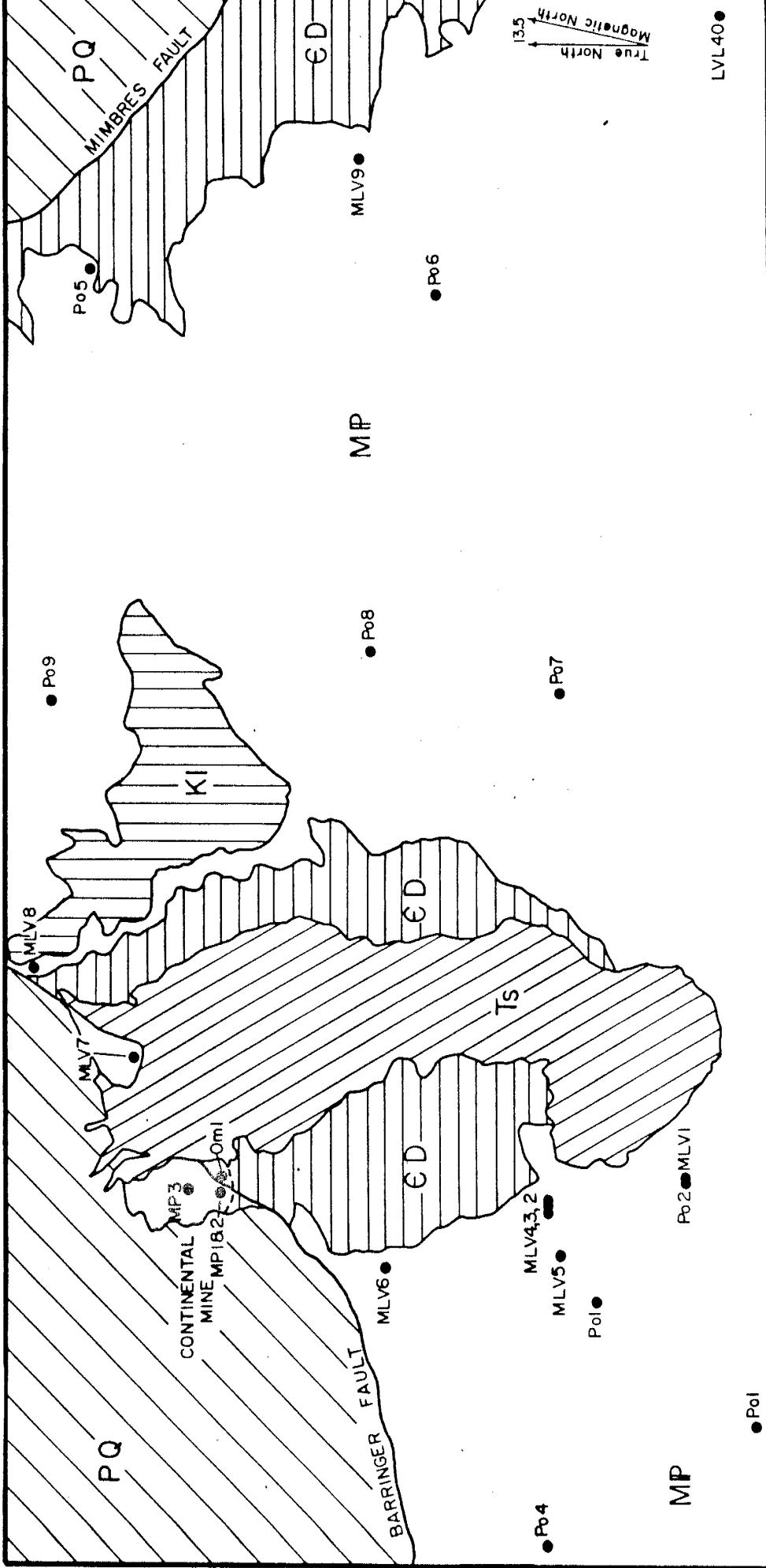
The Continental mine is located in the Central mining district, eastern Grant County, New Mexico. The mine is located along the northwestern margin of the Hanover-Fierro stock (Fig. 3), in the northern portion of the Santa Rita quadrangle.

The Central mining district is located along the northeast flank of a syncline, related to Basin and Range tectonics (Abramson, 1981). Paleozoic sedimentary rocks, Tertiary intrusive rocks, and ore deposits are exposed in the district in a crudely triangular, uplifted block known as the Santa Rita horst (Jones et al., 1967). The Santa Rita horst is bounded by the Barringer Fault to the northeast, the Mimbres Fault to the east (Fig. 3), and a series of discontinuous normal faults to the south.

Figure 3

Generalized geologic map of the northern portion of the Santa Rita Quadrangle, showing major structures and sample locations (after Jones et al., 1967).





LVL40●

1 | 0 | 1 KILOMETER

Disseminated copper deposits, massive iron oxide deposits, and sphalerite replacement deposits are present in the mine (Hernon and Jones, 1967). Copper and sphalerite deposits are concentrated in the Carboniferous Lake Valley Limestone and Oswaldo Formation, and iron oxide deposits are concentrated in the Ordovician Montoya Formation and the Silurian Fusselman Dolomite. Most of the mineralization is located near the Barringer Fault.

Abramson (1981) measured temperatures of homogenization and determined salinities of fluids in garnets and quartz veins collected from the Continental mine. Temperatures of homogenization from 215°C to 435°C were measured in inclusions from garnet. Most of these homogenization temperatures are between 245°C to 345°C, and salinities of these inclusions are from 4.5 to 19.0 eq. wt. % NaCl. Abramson measured temperatures of homogenization from 200°C to greater than 600°C and determined salinities from 2.0 to 47.0 eq. wt. % NaCl in inclusions from quartz. Abramson estimated that temperatures of trapping were at least 30 to 45 degrees higher than temperatures of homogenization measured in her study.

From the analysis of fluid inclusions and rare earth elements Abramson (1981) suggests that the deposit at the Continental mine was formed in two stages; these stages being related to the emplacement of the Hanover-Fierro stock. During middle to late Tertiary time, intrusion of an

equigranular facies metamorphosed the country rock, preparing it for later mineralization. Magmatic waters from a late stage porphyritic facies were transported along the Barringer Fault. These waters leached metals from underlying shales and deposited them in overlying marbles.

METHODS OF INVESTIGATION

SAMPLING

Carbonate rock, silica, and hydrothermally deposited minerals were collected from each deposit for measurement of conodont-color, size of silica-crystallite, and fluid inclusion temperatures. Only carbonate rocks were sampled around each of the deposits because the published conodont CAI, established by Epstein et al. (1977), was assembled from conodonts extracted from carbonate rocks. Approximately four kilograms of carbonate rock were collected at each sample location.

Hansonburg Mining District

Seventy-eight samples of carbonate rock were collected from Pennsylvanian (Des Moinesian-Virgilian) limestones in the Hansonburg mining district. Most of these samples were collected near the Royal Flush-Mountain Canyon, Mex-Tex mines and at Hansonburg Hill (Fig. 1) .

Seventeen samples of carbonate rock were collected near the Royal Flush-Mountain Canyon mines over stratigraphic and lateral intervals. At the Royal Flush mine seven samples were collected over a stratigraphic interval. These samples were collected below the deposit from the Coane and Adobe Formations; from the Council Spring Limestone and Burrego Formation, which host the deposit; and above the deposit from the Story, Del Cuerto, and Moya Formations. These

samples were collected from 9 to 21 meters below the deposit and from 12 to 72 meters above the deposit. Ten samples were collected from the Council Spring and Burrego Formation over lateral intervals near the Royal Flush and Mountain Canyon mines. These samples were collected between 3 to 744 meters from the deposits.

Forty two samples of carbonate rock were collected at the Mex-Tex mine over stratigraphic and lateral intervals. Twenty three samples were collected over stratigraphic intervals from the Bolander Group, Coane and Adobe Formations, Council Spring Limestone, Burrego, Story, Del Cuerto, and Moya Formations. Samples were collected from less than 1 meter to 75 meters above and from less than 1 meter to 75 meters below the deposit. Nineteen samples were collected from the Council Spring and Burrego Formation over lateral intervals near the mineral deposits. These samples were collected from less than 1 meter to 762 meters from the deposit. In addition, one sample of jasperoid (MT1A) and four samples of nodular chert (MT9, MT10, MT11, and MT26) were collected near the Mex-Tex mine. The sample of jasperoid was collected less than 1 meter from hydrothermally deposited quartz (MT1A) and a carbonate sample (MT1). The four samples of nodular cherts were collected within 1 meter of four carbonate samples (MT9, MT10, MT11, MT26) between 33 and 65 meters below the Mex-Tex mine. One sample of hydrothermally deposited quartz (MT1A)

was collected at the Mex-Tex mine for the measurement of fluid inclusion homogenization temperatures. This sample was collected less than 1 meter from carbonate samples MT1 and MT2.

At Hansonburg Hill seven samples of carbonate rock were collected from the Council Spring Limestone over lateral intervals. These samples were collected between 15 and 465 meters from the deposits. One sample of nodular chert (HH1) was collected from the northern portion of Hansonburg Hill, less than 1 meter from carbonate sample HH1. One sample of hydrothermally deposited calcite sample (HH1) was collected for the measurement of fluid inclusion homogenization temperatures. This sample was collected less than one meter from carbonate sample HH1.

Continental Mine-Central Mining District

Twenty-four samples of unmetamorphosed and metamorphosed Mississippian and Pennsylvanian carbonate rocks were collected at and near the Continental mine and areas surrounding the Hanover-Fierro stock (Fig. 3). Two samples of marble and dolomitic marble were collected in the pit of the Continental mine. Additional samples were collected up to 3 kilometers to the east and 5 kilometers to the west in an area surrounding the Hanover-Fierro stock.

One sample of hydrothermally deposited calcite (MP2) and two samples of marble (MP3 and MLV8) were collected from the Continental mine for the analysis of fluid inclusions.

One sample of nodular chert (MP3) was collected from the Continental mine for the measurement of silica crystallite size.

SAMPLE PREPARATION

Conodonts were extracted from carbonate rocks and concentrated using formic acid dissolution, washing and wet sieving, handpicking and mounting techniques described by Brazier (1980). Two of Brazier's preparatory steps were changed for this study to avoid inducing changes in conodont-color. These steps are:

- 1). Cold water was used in preference to hot (80°C) water during formic acid dissolution of carbonate rocks.
- 2). Residues were air dried rather than oven dried after wet sieving.

Mineral specimens were prepared for fluid inclusion microthermometry using methods described by Holland et al. (1978). Cherts were prepared for x-ray diffraction by Dr. Jacques Renault and his assistant using methods described by Renault (1980). Some samples of chert contained both light and dark colored fractions. These fractions were separated from each other and analyzed individually.

ANALYSIS

Conodont Color Alteration

Initially, conodont CAI were determined by comparing conodont colors to the published index chart of Epstein et al. (fig 5., 1977; see Table 1). From personal observations, conodont-color within a given specimen can be perceived differently as a result of the orientation of the sample to the light source, light intensity, magnification, and/or background color. Therefore, a set of conodonts were assembled from field collections and mounted on a neutral gray 18% reflective test card. Conodont CAI from this set were determined by myself and confirmed by independent observers. This collection of conodonts was used as a set of standards for later determinations of CAI.

Conodonts were mounted next to each standard and analyzed under a Nikon binocular microscope. Light intensity, magnification, and orientation of each specimen were held constant throughout measurements of conodont-color.

Classification of conodont CAI was limited to conodonts belonging to the same structural type. In the Central Tennessee mining district only simple cones were compared, and at the Hansonburg mining district and Continental mine only pectinoform elements were measured.

Dimensions of length, width, and height were measured for each conodont element. The volume of each element was roughly determined by using the equation for the volume of a cube.

Some conodonts from Central Tennessee were oxidized or corroded and had a surficial dull, powdery white appearance under the microscope. In these circumstances the conodont specimen was wetted, better revealing its true color (A. Harris, pers. comm., 1984). Conodont colors then were determined following the procedures mentioned above.

Geothermometry

Temperatures of homogenization and melting were measured on a Linkham 600 heating-freezing stage. Greatest emphasis was placed on the examination of primary liquid-vapor inclusions, but some secondary and pseudosecondary inclusions also were studied. Inclusion types were differentiated from each other by methods described by Roedder (1984).

The size of silica-crystallites were measured by Dr. Jacques Renault using methods described by Renault (1980).

RESULTS

HANSONBURG MINING DISTRICT

Recovery

Sixty one kilograms of carbonate rock from the Hansonburg mining district were dissolved in formic acid. One hundred twenty conodonts were recovered from fifty five samples. Sixty eight conodonts were recovered from thirty three samples collected near the Mex-Tex mine. Forty one conodonts were recovered from fifteen samples collected near the Royal Flush mine, and five conodonts were recovered from two samples collected on Hansonburg Hill. Six conodonts were recovered from five samples collected at sites spatially removed from mineralized areas. One to twelve conodonts were recovered from each sample, with an average recovery of two conodonts per sample.

Insoluble residues obtained from the decomposition of limestone samples in formic acid consist of carbonate rock (possibly dolomite?), hydrothermally deposited silica, and minor amounts terrigenous clays. Hydrothermally deposited silica is the dominant residual material recovered from samples collected less than one meter from mineral deposits. Carbonate rock is the most prevalent material recovered from samples collected over one meter from the deposit.

Conodont CAI

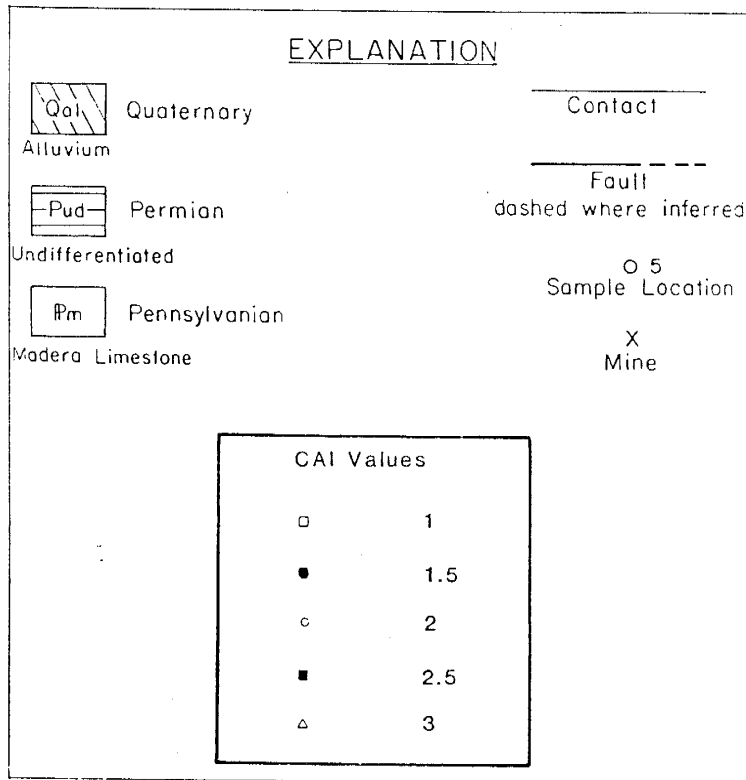
CAI from 1 to 3 were observed in conodonts recovered from samples collected in the Hansonburg mining district (Fig. 4). Conodonts show a wide range of CAI in individual samples collected near the mineral deposits (Figs. 5 and 6). The range of CAI within individual samples diminish away from the deposit, until only values of 1 are present.

Conodont CAI from 1 to 3 were observed in samples collected stratigraphically above and below the mineral deposits at the Mex-Tex and Royal Flush mines (Fig. 5). At the Mex-Tex mine CAI between 1 and 3 were observed in conodonts in samples collected from the Adobe Formation, Council Spring Limestone, Burrego, Story, and Del Cuerto Formations, with 3 being the most prevalent CAI observed in these formations. CAI of 2.5 and 3 are present in strata 48 meters above and 9 meters below the deposit at the Mex-Tex mine. CAI of 1.5 and 2 were the only values observed in conodonts from the Bolander Group, Coane, and Moya Formations. CAI of 1.5 and 2 are present up to 76 meters above and 76 meters below the mineral deposits at the Mex-Tex mine.

Samples collected over stratigraphic intervals near the Royal Flush mine show similar trends in CAI. CAI between 1.5 and 3 were observed in samples collected in the Burrego and Story Formations, up to 30 meters above the deposit, and in samples from the Coane and Adobe Formations, up to 21

Figure 4

Conodont CAI map of the Hansonburg mining district showing distribution of highest CAI in each sample (after Putnam and Norman, 1983).



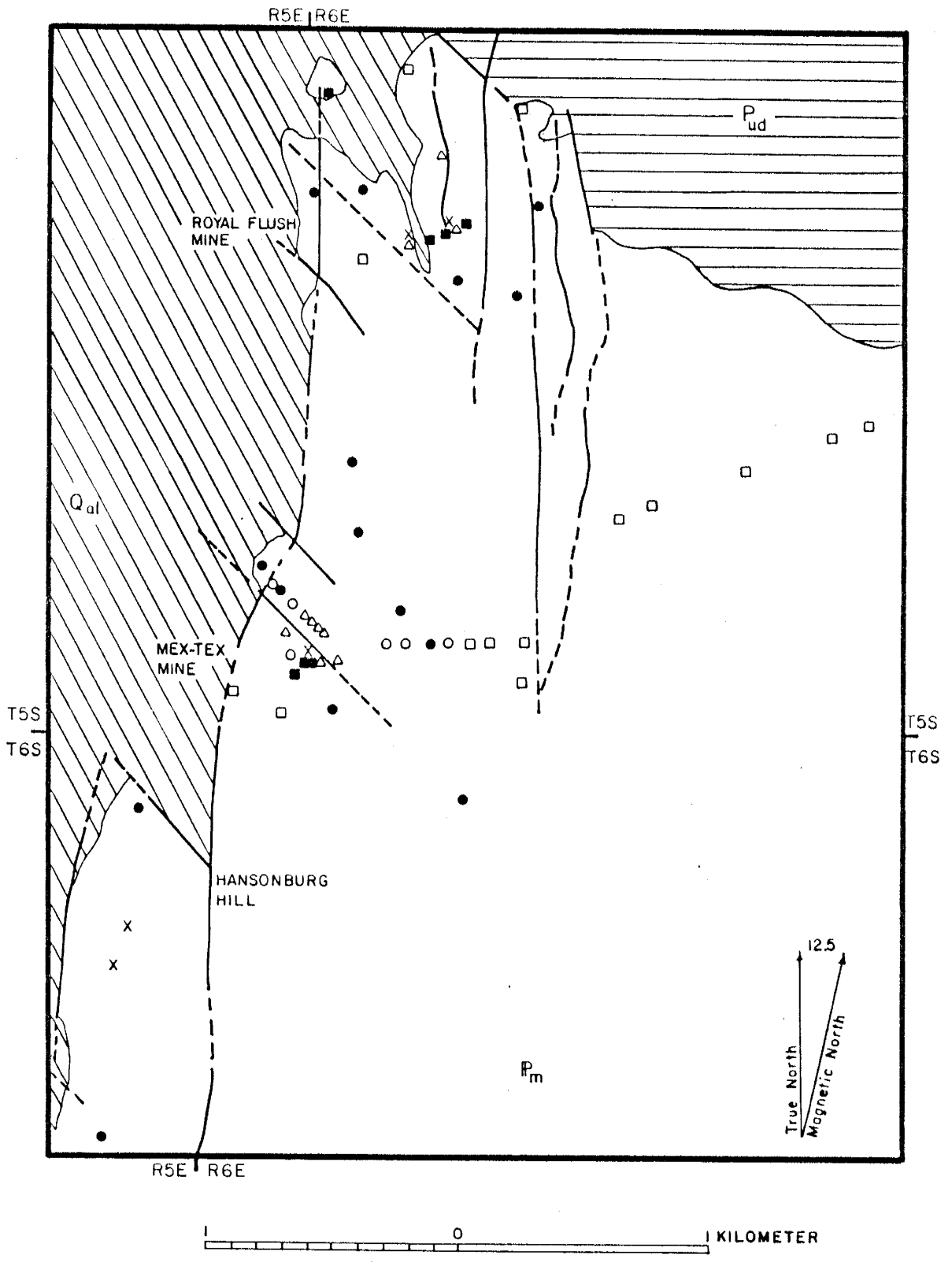


Figure 5

Stratigraphic distribution of CAI in conodonts recovered from samples collected near the Mex-Tex (●) and Royal Flush (▲) mines, Hansonburg mining district.

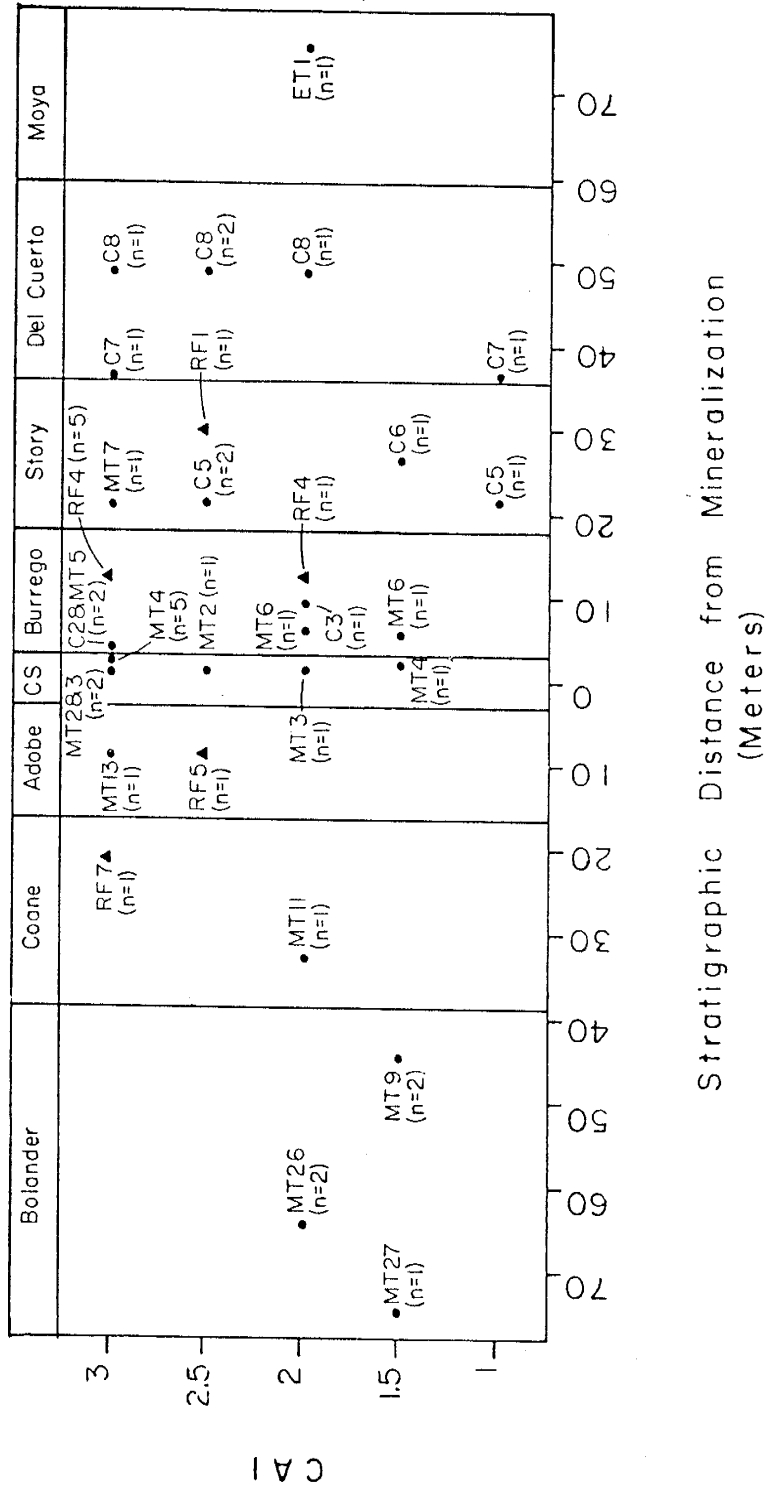
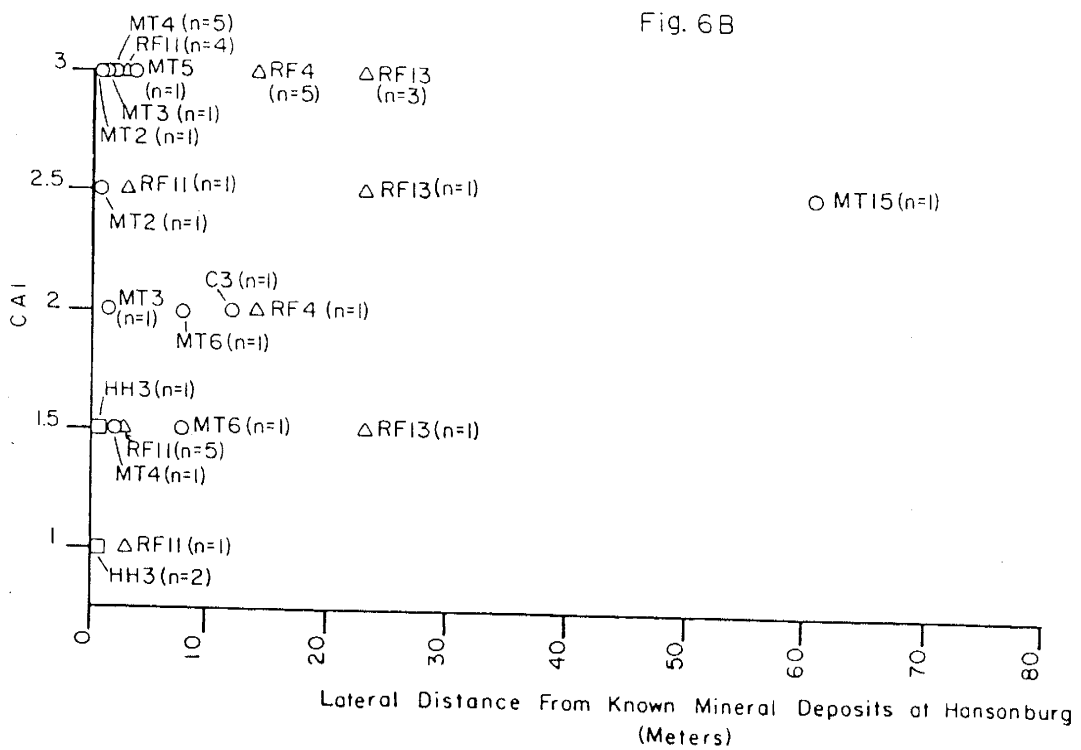
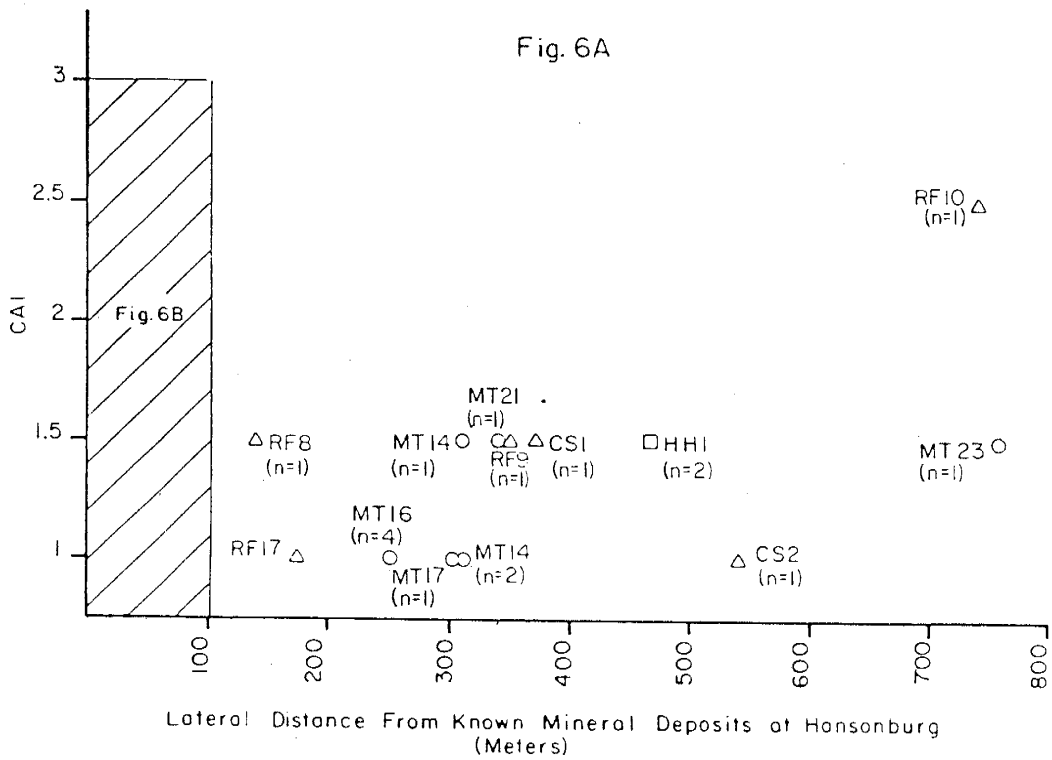


Figure 6

Lateral distribution of CAI in conodonts recovered from samples collected from the Council Spring Limestone and Burrego Formation near the Mex-Tex mine (O), Royal Flush-Mountain Canyon mines (Δ), and at Hansonburg Hill (\square).



meters below the deposit.

CAI from 1 to 3 are present in conodonts recovered from samples collected from the Council Spring Limestone and Burrego Formation over lateral intervals near the mineral deposits at the Mex-Tex and Royal Flush-Mountain Canyon mines and at Hansonburg Hill (Fig. 6). CAI between 1.5 and 3 are present in the Council Spring Limestone and Burrego Formation up to 60 meters from the deposit at the Mex-Tex mine. CAI of 1 and 1.5 were measured in conodonts collected distances greater than 60 meters. At the Royal Flush mine, CAI from 1 to 3 were observed in conodonts recovered from samples collected within 22 meters of the deposit. Except for one sample, RF10, all of the conodonts recovered from samples collected further than 22 meters from the deposit had CAI with 1 and 1.5. Sample RF10 was collected 744 meters from the Royal Flush mine and contained one conodont with a CAI of 2.5.

Conodonts with CAI of 1 and 1.5 were recovered from samples collected on Hansonburg Hill. One of these samples, HH3, was collected from heavily silicified limestones, less than 1 meter from hydrothermally deposited quartz crystals.

Fluid Inclusion Study

Material Studied

Inclusions were analyzed in a quartz sample and a calcite sample collected from the Hansonburg mining district. Primary and some secondary inclusions were examined in each sample. These inclusions consisted of simple two phase liquid-vapor type. The vapor bubble in each inclusion occupies from 7 to 14% of the inclusion's total area.

Primary inclusions in the quartz sample (MT1A) are between 10 to 100 microns in size, with most inclusions greater than 50 microns. These inclusions are isolated from other inclusions and do not show a preferred orientation with other inclusions. Smaller primary inclusions are commonly ovoid and larger inclusions are irregularly shaped.

Secondary inclusions in sample MT1A are less than 50 microns. These inclusions are ovoid and elongated, with their long dimension aligned end to end with neighboring inclusions.

The calcite sample (HHL) consist of irregularly shaped primary inclusions and ovoid secondary inclusions, which are aligned along cleavage planes. These inclusions are between 10 to 100 microns in size.

Temperatures of Homogenization

Results of the distribution of temperatures of homogenization measured in quartz and calcite from the Hansonburg mining district are shown in Figure 7.

Temperatures of homogenization were measured in fifteen inclusions in quartz from the Mex-Tex mine. Temperatures of homogenization from 142oC to 221oC were observed in quartz. Most temperatures of homogenization measured in quartz are between 180oC and 190oC. These temperatures are in agreement with temperatures of homogenization measured in samples from the Hansonburg mining district by Putnam (1980) and Roedder et al. (1968).

Temperatures of homogenization were measured in fourteen inclusions in calcite from Hansonburg Hill. The range of temperatures in these inclusions is from 99oC to 120oC, with most of the homogenization temperatures between 105oC to 115oC.

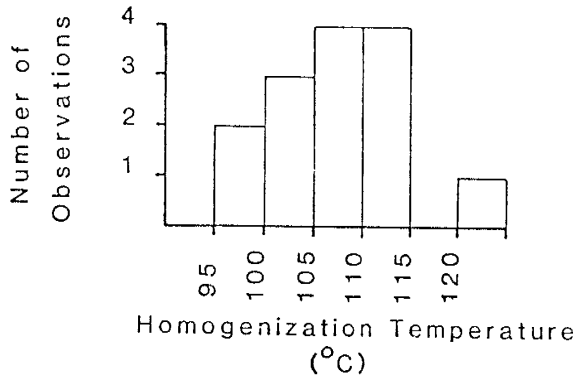
Silica Crystallite Size

Temperatures from 210oC to 222oC were calculated from size of silica-crystallites for five samples of silica collected near the Mex-Tex mine (Table 2).

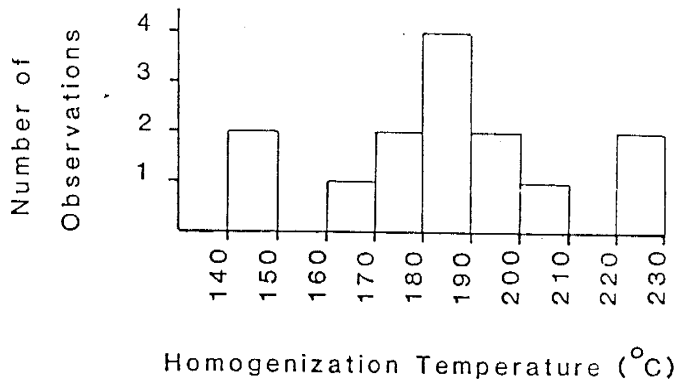
Two measurements of crystallite-size were made in both the light and dark colored fractions of samples MT9, MT10, and HH1. Temperatures within a given sample differ from 5 to 14 degrees.

Figure 7

Histogram of temperatures of homogenization for fluid inclusions in calcite sample HHL (A) and quartz sample MT1 (B).



A



B

Table 2

Temperatures calculated from the size of silica-crystallites for samples of nodular chert and jasperoid collected in the Hansonburg mining district.

SAMPLE NUMBER	SILICA CRYSTALLITE SIZE (A)	TEMPERATURE (°C)
MT-1A	705	222
MT-9 (L)	755	228
MT-9 (L)	641	214
MT-9 (D)	612	210
MT-9 (D)	560	203
MT-10	674	218
MT-11	710	222
MT-26	687	220
HH-1 (L)	645	215
HH-1 (L)	608	210
HH-1 (D)	546	201
HH-1 (D)		214

Note: D=Dark Fraction; L=Light Fraction

CONTINENTAL MINE

Recovery

Sixteen kilograms of carbonate rock collected near the Continental mine and Hanover-Fierro stock were digested in formic acid. Thirty one conodonts were recovered from eleven samples. Conodonts were not recovered from samples collected from the pit of the Continental mine. Thirteen conodonts were recovered from samples collected from the Lake Valley Formation, and eighteen conodonts were recovered from samples collected from the Oswaldo Formation. Each sample contained one to nine conodonts, with an average of three conodonts per sample.

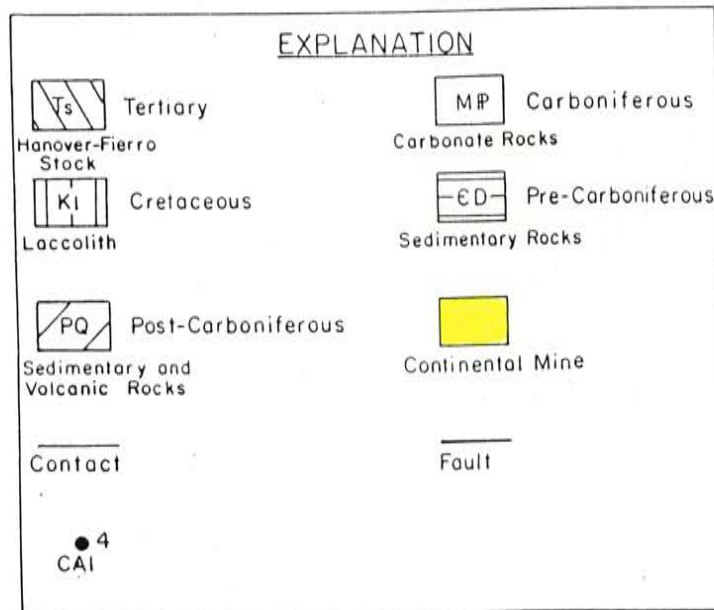
Insoluble residues consist principally of carbonate rock (limestone and marble), terrigenous rounded to subrounded sand grains, and hydrothermally deposited magnetite. Marble and magnetite are the dominant constituents recovered from samples collected in the open pit of the Continental mine. Carbonate rock is the dominant residual material recovered from samples collected outside the pit.

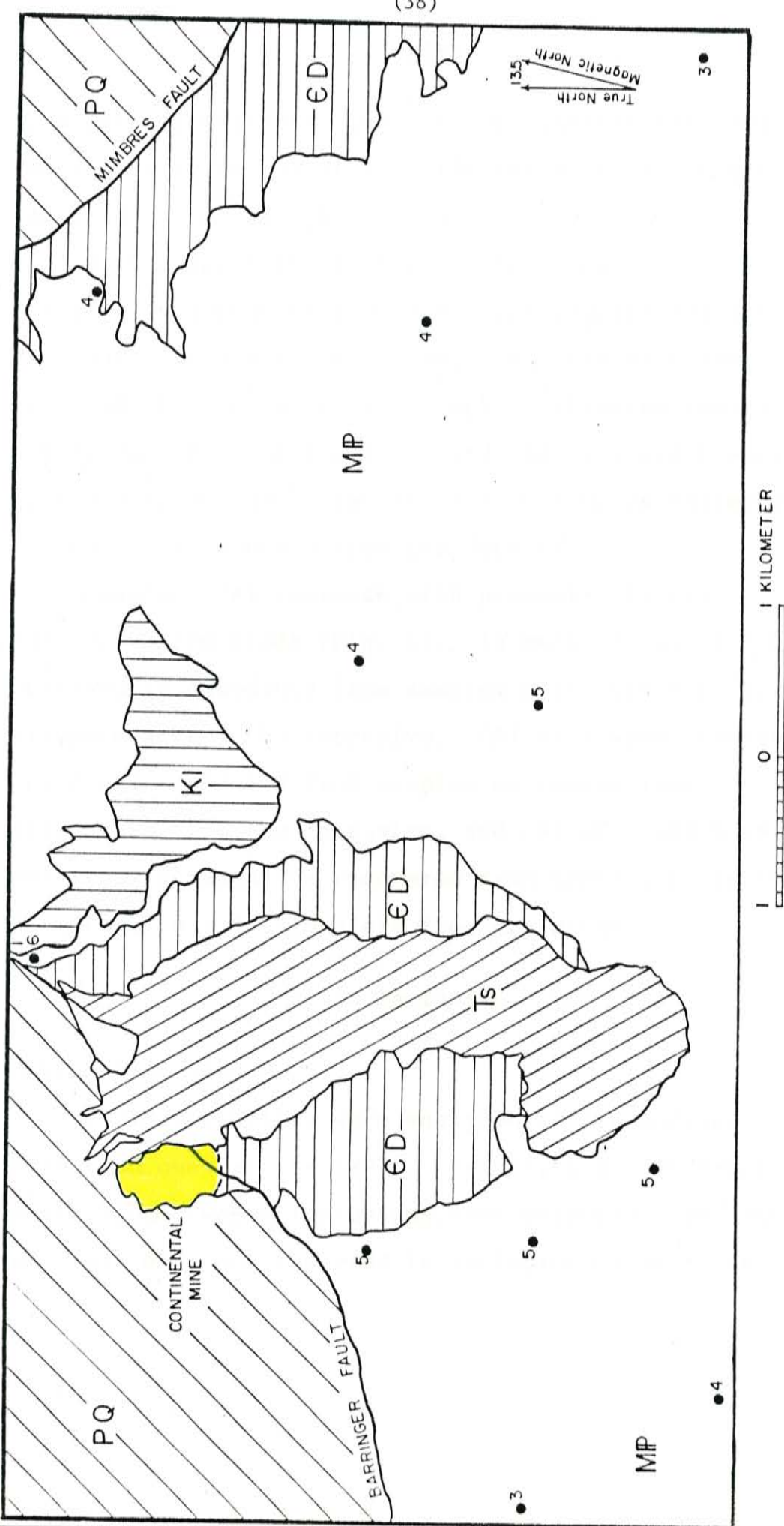
Conodont CAI

Conodont CAI from 3 to 6 were observed in conodonts recovered from samples collected near the Continental mine and Hanover-Fierro stock (Fig. 8). Unlike the conodonts recovered from the Hansonburg mining district, conodonts

Figure 8

Conodont CAI map in the northern portion of the Santa Rita quadrangle (after Jones et al., 1967).





from samples collected near the Continental mine and the stock usually do not show a wide range of CAI in conodonts recovered from the same sample.

With respect to the Continental mine, CAI of 3 were observed in conodonts recovered from samples collected from 3.0 to 8.2 kilometers from the mine. CAI of 4 were observed in conodonts recovered from samples collected from 3.8 to 6.0 kilometers from the mine, and CAI of 5 and 6 were observed in conodonts recovered from samples collected from 1.5 to 3.7 kilometers from the deposit.

Conodont CAI increase with proximity to the Hanover-Fierro stock (Fig. 9). In general CAI of 3 were observed in conodonts from samples collected from 2.2 to 6.2 kilometers from the intrusive. CAI of 4 were observed in conodonts recovered from samples collected from 1.5 to 4.4 kilometers from the intrusive, and CAI of 5 and 6 were observed in conodonts recovered from samples collected from 30 meters to 1.5 kilometers from the stock.

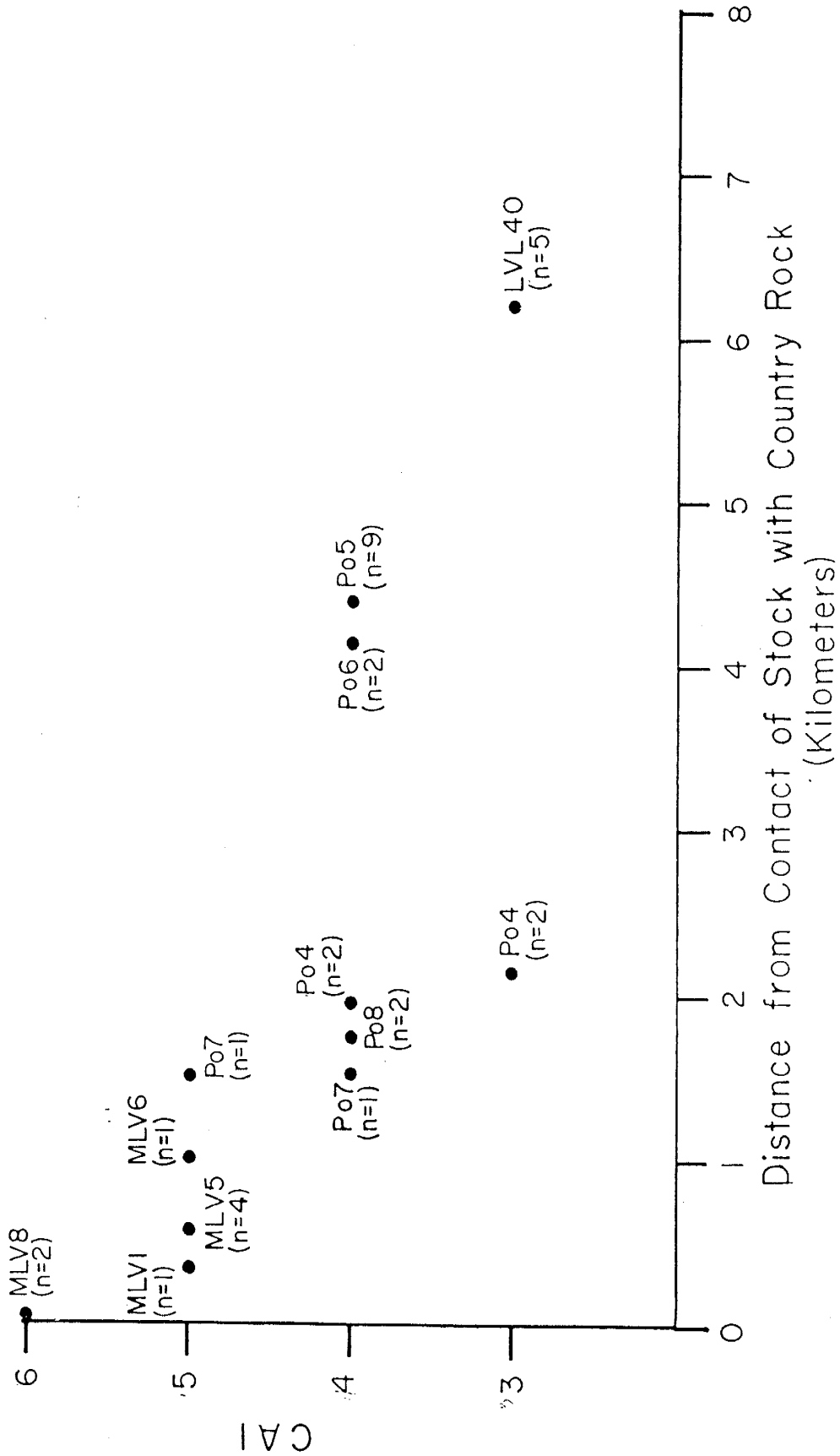
Fluid Inclusion Study

Material Studied

Fluid inclusions were analyzed in two marbles (MP3 and MLV8) and one calcite (MP2). Primary and some secondary two phase liquid-vapor inclusions were measured. Daughter minerals were not observed in inclusions from these samples.

Figure 9

Distribution of CAI in conodonts collected near the Hanover-Fierro stock.



Inclusions in all samples were less than 50 microns. These inclusions were ovoid in shaped and aligned end to end with other inclusions. Primary inclusions were differentiated from secondary inclusions by their differences in temperatures of homogenization.

Temperatures of Homogenization

Temperatures of homogenization were measured in eight inclusions from marble (MP3), thirteen inclusions in calcite (MP2), and thirteen inclusions from marble (MLV8). Results of these measurements are illustrated in Figure 10.

Temperatures of homogenization from 202°C to 334°C were measured in inclusions from samples MP3 and MP2.

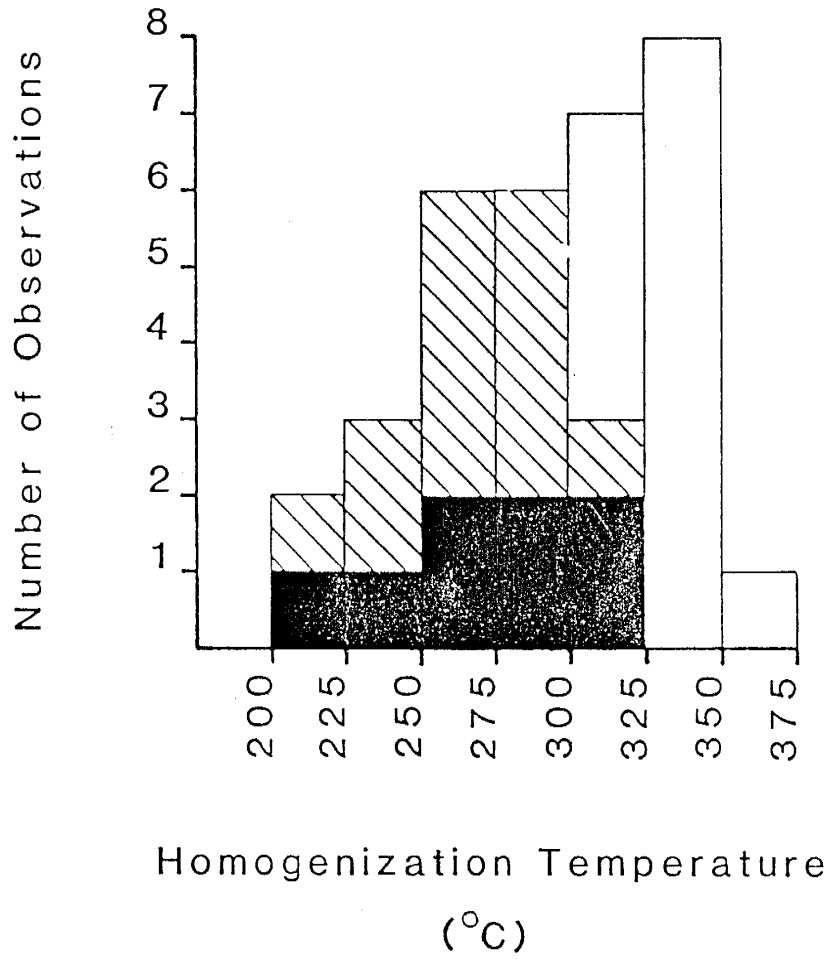
Temperatures of homogenization from 300°C to 351°C were measured in inclusions from sample MLV8. These measurements are in agreement with temperatures of homogenization measured by Abramson (1981).

Silica Crystallite Size

Only one chert was analyzed from the Continental mine. This sample was collected in the pit of the mine. An unreasonably high temperature was determined for this sample, but it was so intensely recrystallized that the calculated temperature was meaningless in this context.

Figure 10

Histogram of temperatures of homogenization for inclusions in samples MP2 (diagonal lines), MP3 (shaded), and MLV8 (unshaded) from the Continental mine.



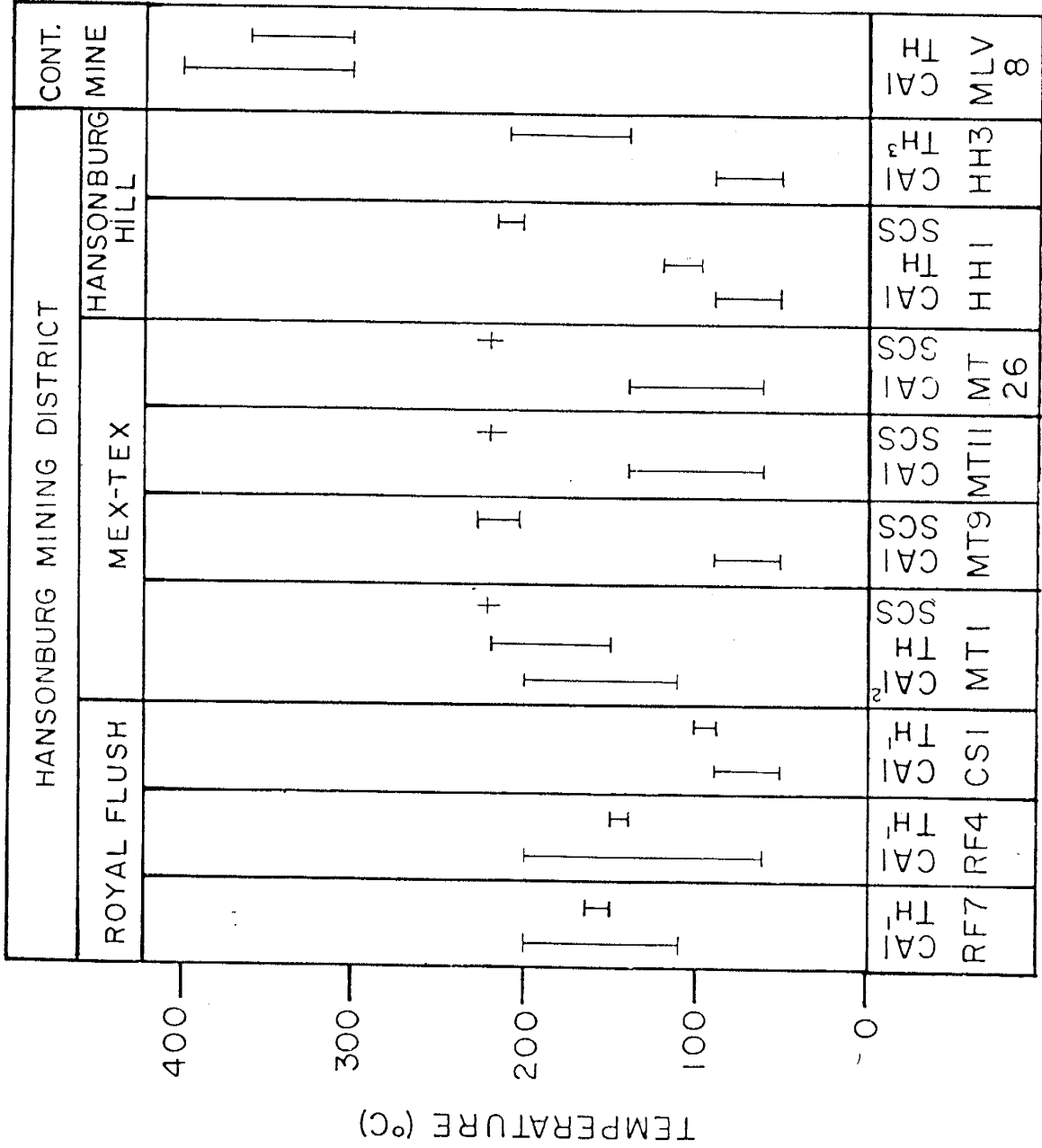
CONFIRMATION OF ASSUMPTIONS

I have assumed that the temperature scale developed by Epstein et al. (1977) relates conodont CAI to specific temperatures. Figure 11 is a comparison between Epsteins' proposed range of temperatures for CAI, temperatures of homogenization for fluid inclusions in minerals collected less than one meter from conodont sample localities, and temperatures calculated from the size of silica-crystallites. Figure 11 shows that, with the exception of sample HH3, temperatures determined by Epstein et al. (1977) show a close correlation to fluid inclusion homogenization temperatures in the Hansonburg mining district and Continental mine. Figure 11 also shows that, with the exception of sample MT1, temperatures determined from the size of silica-crystallites are higher than temperatures related to conodont CAI and fluid inclusion homogenization temperatures. From these observations, I contend that the temperature scale developed by Epstein et al. (1977) reflects temperatures associated with CAI in the Hansonburg mining district and at the Continental mine.

I have also assumed that the alteration of conodont-color is independent of conodont-size. A chi-square test was used to test the relative independence of these two properties. The chi-square test is a goodness-of-fit test which compares empirical and theoretical distributions by way of contingency tables (Table 3).

Figure 11

Comparison of temperatures related to conodont CAI (Epstein et al., 1977)(CAI), fluid inclusion homogenization temperatures (TH), and temperatures determined from the diameter of silica-crystallites (SCS). Bars represent a range of temperatures and plus signs represent a single temperature.



¹Measured by W. Ting

²From Sample MT2

³From Putnam and Norman (1983)

Table 3

Contingency table of conodont CAI versus size of conodonts recovered from the Hansonburg mining district and the northern portion of the Santa Rita quadrangle.

CAI	VOLUME ($\times 10^{-3}$ mm ³)		SUM OF ROWS
	0-3.99	> 3.99	
1	28 (19.62)	9 (17.38)	37
1.5-2	19 (18.56)	16 (16.44)	35
2.5-3	11 (19.09)	25 (16.91)	36
4-6	12 (12.73)	12 (11.27)	24
SUM OF COLUMNS	70	62	132

CHI-SQUARE = 15.03

DEGREES OF FREEDOM = 3

NOTE: Theoretical values in parentheses

If the property being tested (in this case CAI) is independent of a condition (size of conodont) then ideally the observed distribution should be equal to the theoretical distribution, and chi-square should equal zero. The degree of independence is determined from chi-square probability tables and reported as confidence intervals. In this study a 4-by-2 contingency table was constructed comparing conodont CAI from Hansonburg and Continental mine to the volume of these conodonts (Table 3). The chi-square calculated from the contingency table is 15.03. From chi-square probability tables (Koch and Link, 1970), this number indicates that probability of independence between conodont CAI and volume is less than 0.5%. Therefore, independence is rejected. Results from the chi-square test suggest that color-alteration in the Hansonburg mining district and Continental mine is not solely attributable to temperatures related to hydrothermal activity, and color-alteration is strongly dependent upon conodont-size.

I also assumed that conodonts examined in this study were not removed from their original sites of deposition by processes of reworking and stratigraphic leakage. Reworked fossils can be discerned on an empirical basis by their mode of preservation and their environment of deposition. Conodonts recovered from the Hansonburg mining district and Continental mine did not show signs of abrasion or weathering. These conodonts were recovered from micritic

limestone. Deposition of micrite requires relatively quiescent, low-energy conditions (Folk, 1959). Transportation of conodonts requires moderate to high energy environments because the specific gravity of conodonts is between 2.84 and 3.10 (Ellison, 1944). The association of dense conodonts in micritic limestones suggests that the conodonts from the Hansonburg mining district and Continental mine were deposited in situ.

A stratigraphic leak is defined as the deposition of fossils of younger age into older aged material (Foster, 1966). Solution channelways, resulting from the dissolution of limestone or zones of structural weakness, commonly serve as avenues of transport for stratigraphic leaks. I contend that conodonts observed in this study were not leaked from younger rocks because samples of limestones were not collected in fault gouge or in areas characteristic of dissolution zones, such as brecciated limestones. Furthermore, the presence of stratigraphic leaks in samples from the Hansonburg mining district and Continental mine is unlikely because, with the exception of Permian San Andres Limestone and Yeso Formation, Permian and Triassic strata in the study areas resulted from deposition of sediments in non-marine environments, which were not conducive to conodont life.

INTERPRETATION

Hansonburg Mining District

To determine whether anomalous CAI were observed in conodonts from the Hansonburg mining district, background CAI were first estimated. These background values represent the cumulative effects of heating from sources other than temperatures related to mineralization. The most common sources of heat in geologic systems are related to depth of burial and igneous activity. Other than a quartz monzonite dike located on Hansonburg Hill, the closest known igneous rocks occur near Socorro, New Mexico (64 kilometers to the west), near Carrizozo, New Mexico (48 kilometers to the east), and near the Capitan Lineament (16 kilometers to the north). Therefore, temperatures related to depth of burial are the most probable cause for background temperatures in the district.

Temperatures of burial can be calculated if the thickness of overburden and geothermal gradient are known. Based on field observations, Allmendinger (1975) and Wilpolt and Wanek (1951) estimated that Pennsylvanian rocks in south-central New Mexico were buried by 1.5 to 2 kilometers of upper Paleozoic and Mesozoic rocks. Based on fluid inclusion data Norman et al. (1985) suggest that early Tertiary fluids responsible for mineral deposition were subjected to pressures between 150 to 200 bars. Under hydrostatic pressure, 150 to 200 bars is compatible with the

depth of burial suggested by Allmendinger (1975) and Wilpolt and Wanek (1951).

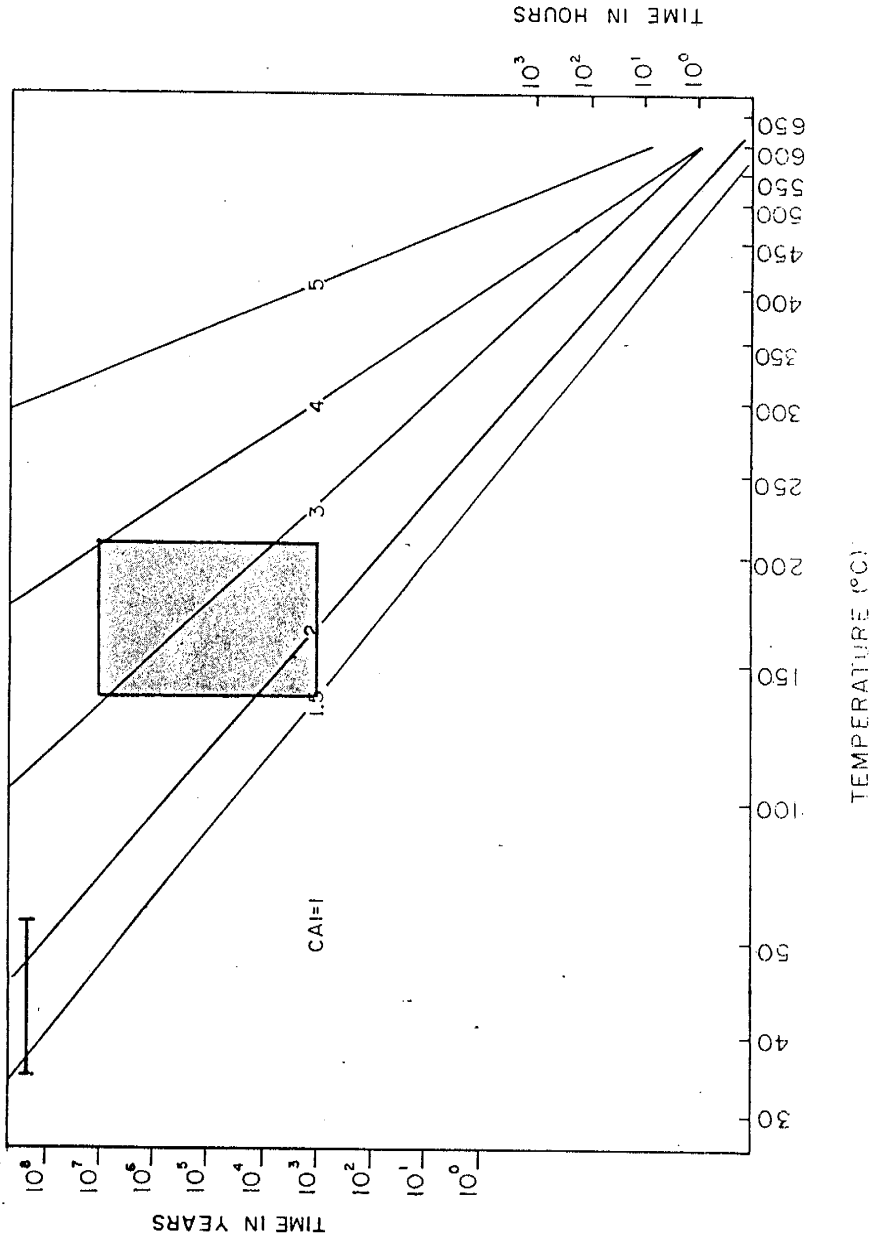
Assuming an average geothermal gradient of $33^{\circ}\text{C}/\text{km}$ ($1^{\circ}\text{C}/100\text{ ft}$) temperatures between 50°C and 66°C would be predicted to occur at depths of 1.5 to 2 kilometers. Present day geothermal gradients between $26^{\circ}\text{C}/\text{km}$ and $29^{\circ}\text{C}/\text{km}$ were measured in drill holes near the Hansonburg mining district (Reiter et al., 1975), suggesting temperatures between 33°C and 58°C for these depths.

Based on the Arrhenius plot published in Epstein et al. (1977, fig. 3), CAI of 1, 1.5, and 2 would be predicted to occur in conodonts subjected to temperatures between 33°C and 66°C over an interval of 280 million years (Fig. 12). CAI of 1, 1.5 and 2 are present in conodonts collected in the district. CAI of 1 is the most widely distributed CAI, and CAI of 1 is the only CAI present in conodonts recovered in samples collected furthest from the mineral deposits. Based on my observations I suggest that CAI of 1 represent background values in the Hansonburg mining district.

CAI of 1.5 and 2 are located between CAI of 1 and CAI of 2.5 and 3 (Fig. 4). W. Ting (pers. comm. , 1984) measured fluid inclusion temperatures of homogenization in limestone collected less than 6 meters from the present studies sample locations. Temperatures of homogenization progressively decrease away from the mineral deposit at the Royal Flush mine. Salinities of 10 eq. wt. % NaCl

Figure 12

Arrhenius plot of temperature versus time, showing predicted CAI associated burial (bar) and CAI related to the deposition of hydrothermal minerals (shaded) in the Hansonburg mining district (after Epstein et al., 1977).



determined by Ting for these inclusions are similar to salinities between 10 and 15 eq. wt. % NaCl for inclusions in fluorite and quartz from the Royal Flush mine (Roedder et al., 1968, Putnam and Norman, 1983). The correlation between Ting's fluid inclusion study and temperatures related to CAI in the present study (Fig. 11) suggest that CAI of 1.5 and 2 may have resulted from the alteration of conodont-color by low temperature hydrothermal fluids compositionally similar to fluids responsible for mineral deposition at the Royal Flush mine.

CAI of 2.5, and 3 are localized around the mineral deposits and faults at the Mex-Tex and Royal Flush mines (Fig. 4), with 3 being closest to the mineralization. Temperatures between 110°C and 200°C determined by Epstein et al. (1977) for CAI of 3 are similar to fluid inclusions homogenization temperatures for the Hansonburg mining district in the present study (Fig. 11), by Putnam and Norman (1983), and by Roedder et al. (1968).

Roedder (1960) set general time constraints for the deposition of Mississippi Valley-type deposits from 1 thousand to 10 million years, depending upon the concentration of metals in solution and the rate of flow of hydrothermal solutions. The Arrhenius plot (Fig. 12) published in Epstein et al. (1977) predicts that continuous heating between 140°C and 210°C for 1000 years will give a CAI of 2, and continuous heating between these temperatures

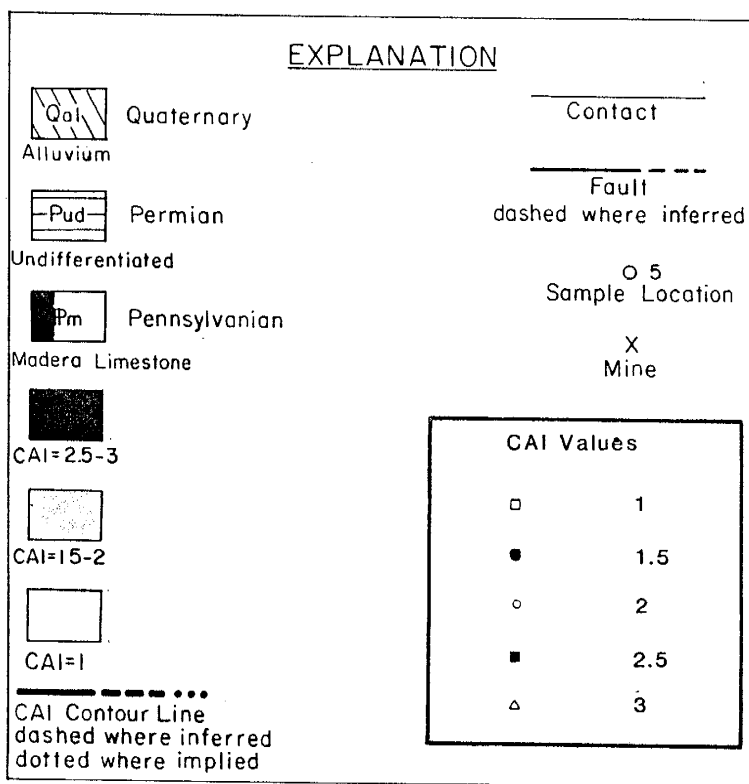
for 10 million years will give a CAI of 3 or 4. Based on these observations I conclude that CAI of 2.5 and 3 observed in conodonts recovered from samples near mineral deposits at the Hansonburg mining district resulted from temperatures related to mineralization.

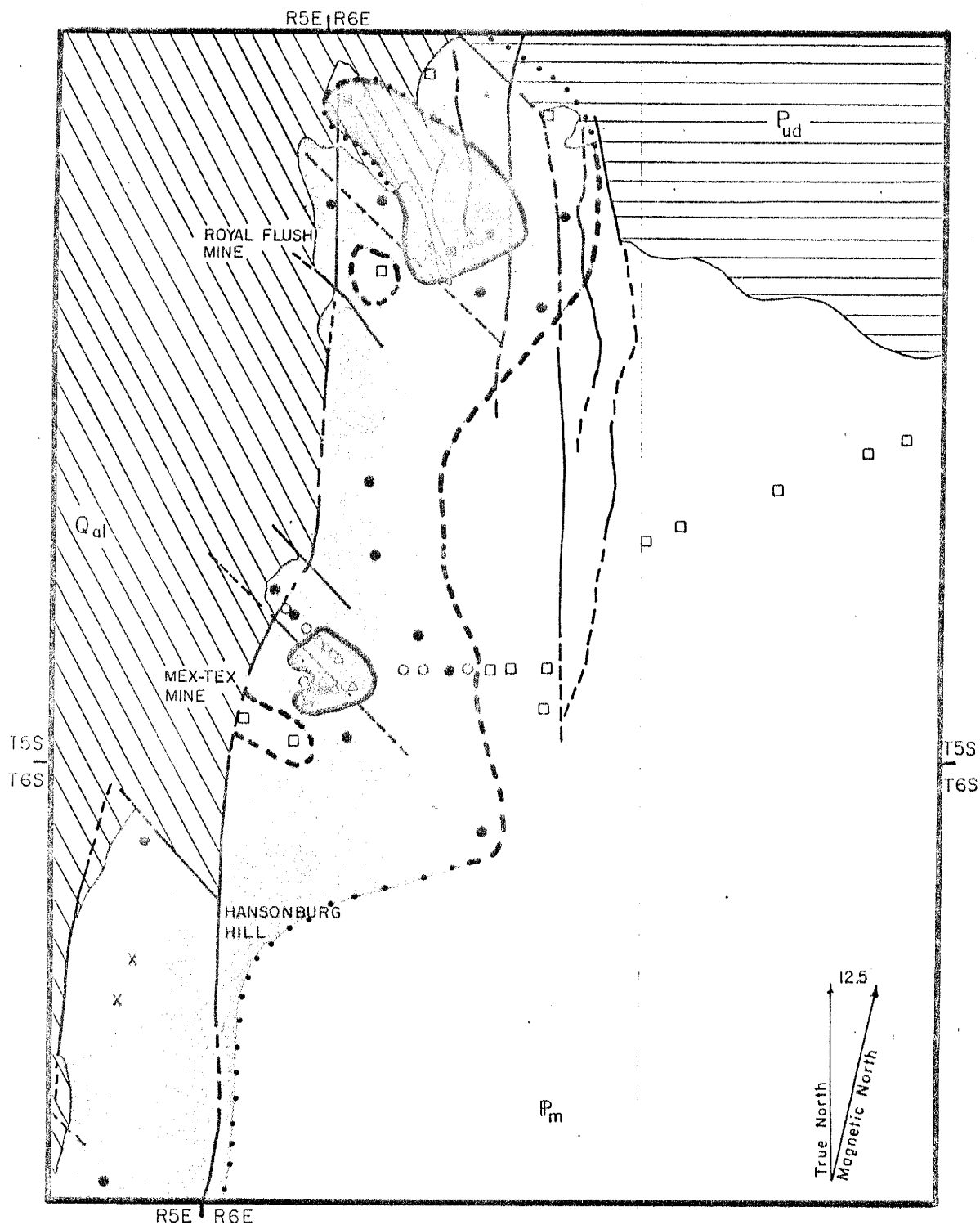
There are exceptions. CAI of 2.5 and 3 were not observed in one sample (HH3) which was collected near hydrothermally deposited quartz on Hansonburg Hill. Putnam and Norman (1983) measured fluid inclusion homogenization temperatures from 125°C to 210°C in inclusions from quartz samples collected from this area. This indicates that conodonts recovered from sample HH3 were not similarly affected by hydrothermal activity in this area.

Figure 13 is a conodont CAI contour map showing the orientation and extent of thermal aureoles near the mineral deposits in the Hansonburg mining district. This map shows three levels of discrimination; 1, 1.5 to 2, and 2.5 to 3. CAI of 2.5 and 3 show localized, northwest-trending thermal aureoles around the mineral deposits at the Royal Flush-Mountain Canyon and Mex-Tex mines. Intermediate values of 1.5 and 2 are regionally widespread throughout the district. The extent of these anomalous values coupled with fluid inclusion data suggest that large volumes of hydrothermal fluids infiltrated the country rock. The exchange of heat from these hydrothermal fluids to conodonts resulted in the alteration of conodont-color from background

Figure 13

Conodont CAI contour map showing the extent of anomalous CAI in the Hansonburg mining district (after Putnam and Norman, 1983).





values of 1 to present values from 1.5 to 3.

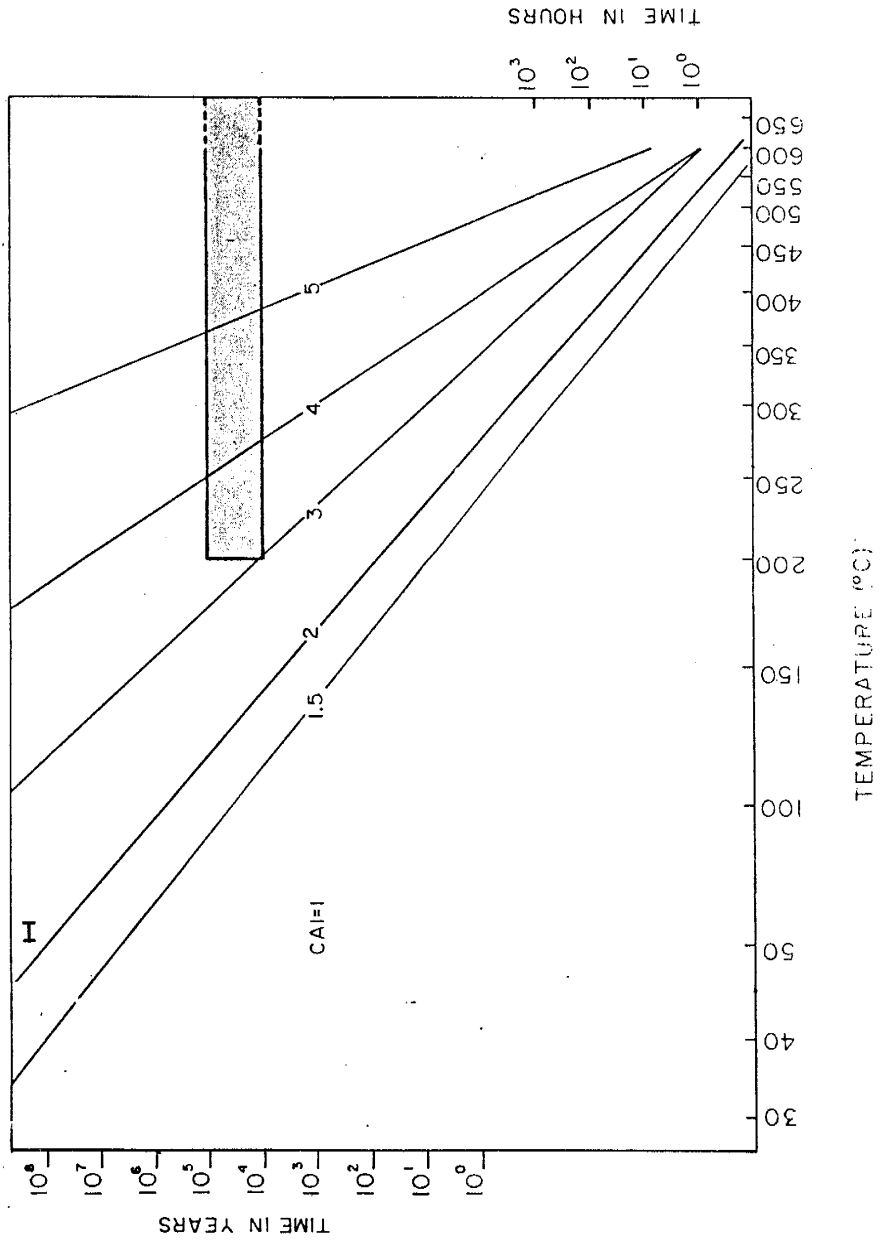
Continental Mine

According to Jones et al. (1967), a sediment pile at least 2 kilometers thick may have overlain the Lake Valley Formation and Oswaldo Formation in the vicinity of the Continental mine. The present day geothermal gradient between $25^{\circ}\text{C}/\text{km}$ and $30^{\circ}\text{C}/\text{km}$ was calculated using Fourier's Law of heat conduction, and heat flow data from Swanberg (1980) and Rieter and Tovar (1982). Temperatures between 52°C and 60°C should be present at a depth of 2 kilometers, assuming a geothermal gradient between $25^{\circ}\text{C}/\text{km}$ and $30^{\circ}\text{C}/\text{km}$. Based on the published Arrhenius plot from Epstein et al. (1977) CAI of 2 would be predicted to occur in conodonts subjected to temperatures between 52°C and 60°C for an interval of 280 million years (Fig. 14). CAI of 2 were not observed in conodonts collected in the area surrounding the Continental mine and Hanover-Fierro stock (Fig. 8). The presence of Tertiary igneous rocks near the Continental mine suggests that the geothermal gradient was much higher in the past.

Fluid inclusion homogenization temperatures greater than 200°C are associated with mineral deposition and skarn formation at the Continental mine (Abramson, 1981). Abramson suggested that skarn formation and mineral deposition were related to the emplacement of the Hanover-Fierro stock. According to Cathles (1977, 1981),

Figure 14

Arrhenius plot of temperature versus time showing predicted CAI associated burial (bar) and CAI related to temperatures of skarn formation and mineral deposition (shaded) near the Continental mine (after Epstein et al., 1977).



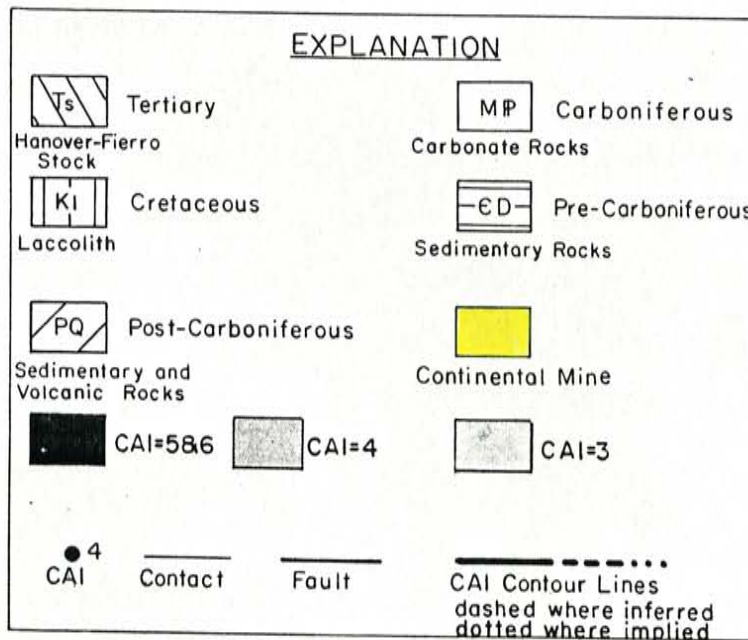
cooling of a magmatic body to 25% of its initial temperature would require a period of time between 10 thousand years and 100 thousand years. CAI of 3 or greater would be predicted to occur at fluid inclusion homogenization temperatures greater than 200°C over a period of time spanning 10 thousand to 100 thousand years (Fig. 14).

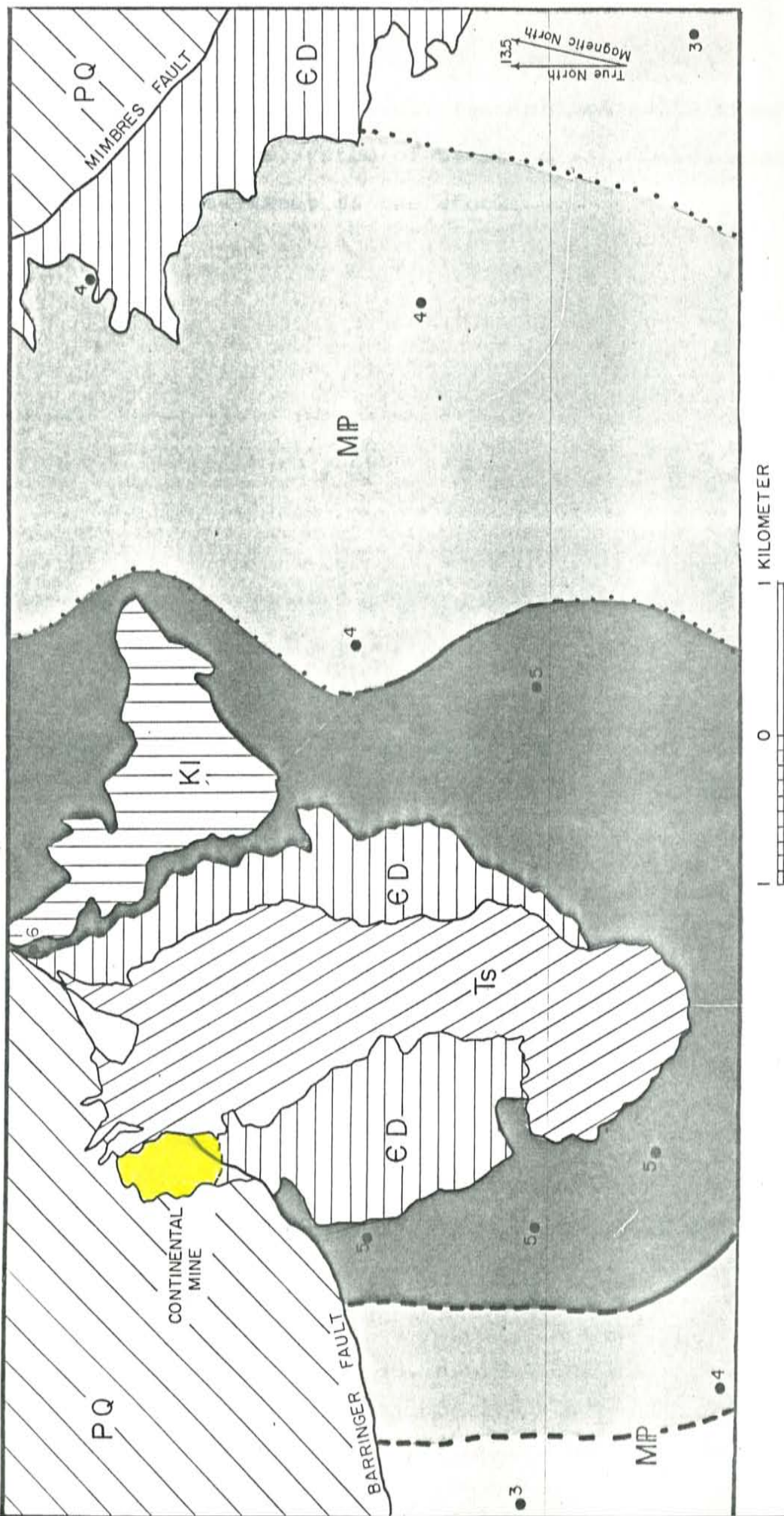
CAI of 3, 4, 5, and 6 were observed in conodonts surrounding the Hanover-Fierro stock. The extent of these anomalous values suggest that a regional thermal anomaly existed which was associated with the stock (Fig. 15). The distribution of CAI near the Continental mine does not clearly show the location of mineralized zones because the intense thermal effects associated with emplacement of the Hanover-Fierro stock extend beyond these mineralized zones (Abramson, 1981).

Lovering (1935) and Jaeger (1957,1959) showed that temperatures related to magmatic activity decrease to 10% of an intrusives initial temperature within 1 kilometer when conduction of heat through country rock is the only mechanism responsible for transmitting heat outside of the intrusive. Cathles (1977, 1981) showed that the transmission of heat by the convection of groundwater near an intrusive can affect an area within 10 kilometers of that magmatic body. Based on these works and my observations I propose that the wide areal extent of anomalous CAI surrounding the Hanover-Fierro pluton resulted from elevated

Figure 15

Conodont CAI contour map of the northern portion of the Santa Rita quadrangle showing extent of thermal anomaly around the Hanover-Fierro stock (after Jones et al., 1967).





temperatures in a relatively short-lived (<100 thousand years) convective system of hydrothermal fluids associated with the emplacement of the stock.

APPLICABILITY OF METHOD

Using conodont CAI to delineate thermal aureoles around mineral deposits in the Hansonburg mining district was successful for two reasons. First, CAI associated with hydrothermal activity was appreciably higher than CAI related to background temperatures. Second, CAI progressively increase from 1 to 3 with proximity to the mineral deposits in the district.

The progressive increase in CAI from 1 to 3 with proximity to the deposits can serve as a directional indicator towards the locus of mineralization. A conodont CAI contour map, similar to the one illustrated in Figure 13, might be used to determine this proximity to other mineral deposits in the Hansonburg mining district. Given the specific conditions of mineralization for Hansonburg, CAI of 2.5 to 3 should indicate a relatively high probability of the presence of a mineral deposit within approximately 100 meters. CAI of 1.5 to 2 suggest that mineral deposit might be present within an area of 400 meters, and CAI of 1 indicate an extremely low probability of the presence of a mineral deposit nearby. Using these parameters, the conodont CAI contour map (Fig. 13) constructed in the present study suggest that additional mineralization might be located northwest of the Royal Flush mine.

Anomalous CAI observed in the vicinity of the Continental mine did not successfully distinguish a local thermal anomaly directly associated with the mineral deposit, but these CAI did delineate a regionally extensive thermal aureole associated with the Hanover-Fierro pluton. Although this technique did not pinpoint the location of the mineral deposit at the Continental mine, it can still be used to delineate large areas affected by hydrothermal fluids associated with igneous activity, especially if mineralization is believed to be associated with an intrusive or if the intrusive is buried.

CENTRAL TENNESSEE MINING DISTRICT

Introduction

Examination of CAI in conodonts from the Hansonburg mining district and Continental mine indicates that conodont-color is affected by hydrothermal activity related to mineral deposition, and that the distribution of CAI in these districts can be used to locate the source of a heating event. Conodonts from the Central Tennessee mining district were studied to determine whether the distribution of CAI might be used to locate an unexposed mineral deposit.

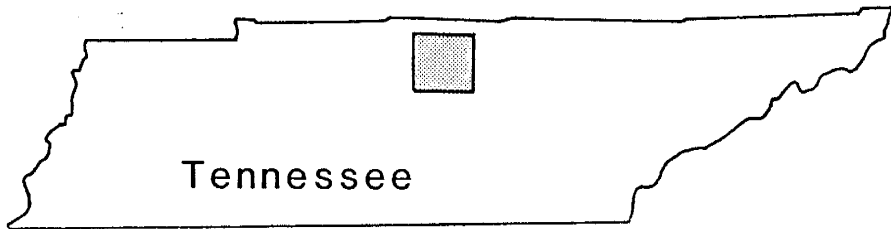
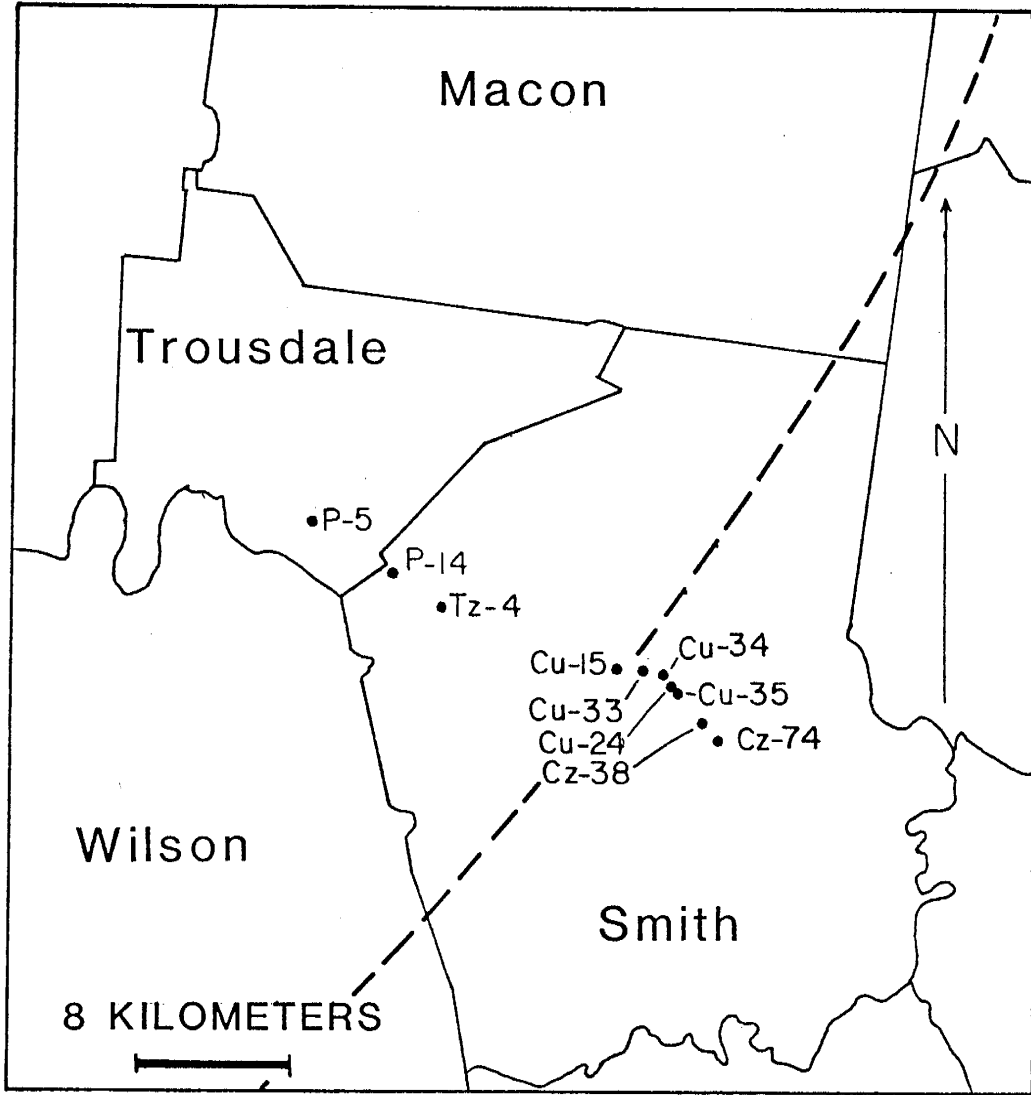
Geologic Setting

The Central Tennessee mining district is located in Smith and Truesdale Counties, Tennessee (Fig. 16). Rocks in the mining district consist of Cambrian through Mississippian sedimentary rocks. Carbonate rocks are the dominant lithology in the district, and clastic rock comprise the remaining portion of the lithology present in the area.

The Cincinnati Arch is the major structural feature in the region. Its axis trends northeastward bisecting Smith County (Fig. 16). Strata gently dip away from the crest of the arch, with a regional dip of less than one degree (Kyle, 1973).

Figure 16

General location and drill site location map of the Central Tennessee mining district. Dashed line represents the axis of the Cincinnati Arch (after Kyle, 1973).



Mineralization in the district is scattered laterally and stratigraphically in the karstified, Lower Ordovician Knox Dolomite (Fig. 17). Sphalerite is the only mineral mined in the district. Fluorite, barite, calcite, dolomite, and galena are also present (Kyle, 1973).

Roedder (1971) measured temperatures of homogenization and melting of fluid inclusions in sphalerite, fluorite, and barite from the district. Temperatures of melting measured by Roedder are between -7.5°C to -30.0°C , with most temperatures near -20.0°C . Roedder (1971) noted that measured temperatures of first melt below -28.0°C is suggestive of the presence of calcium chloride in these inclusions. Temperatures of homogenization, measured by Roedder, were between 50°C to 140°C , with most temperatures near 110°C . Roedder estimated that temperatures of trapping were less than ten degrees higher than temperatures of homogenization.

DeGrootdt (1973) measured temperatures of homogenization between 64°C to 151°C for inclusions in fluorite. The range of most of these measurements is between 90°C to 120°C .

Hoagland (1976) suggests that middle Ordovician shales in the Appalachian Basin are source rocks for the zinc in the district. He suggests that in Late Paleozoic time hydrothermal metal-bearing fluids were driven out of the basin as a result of compaction of these argillaceous sediments. Hoagland (1976), Kyle (1973), and Harris (1971)

Figure 17

Profile showing sample locations (■) and distribution of mineralization (rectangles on right side of each core) in drill cores from the Central Tennessee mining district.

contend that the karstified Knox Dolomite acted as a conduit for these fluids. Braun (1983) proposed that sphalerite precipitated in paleodomes below aquicludes where metal-bearing, hydrothermal solutions interacted with hydrocarbons and other reductants.

Sampling

Thirty samples of carbonate rock from the Central Tennessee mining district (Fig. 17) were collected from ten drill cores by Bruce Ahler and Jay Gregg of St. Joe Minerals Corporation. Fluorite and sphalerite also were obtained from some of these samples for fluid inclusion studies and samples of nodular chert were obtained for the measurement of crystallite size.

RESULTS

Recovery

Thirty two kilograms of carbonate rock from the Central Tennessee mining district were dissolved in formic acid. Twenty six conodonts were recovered from sixteen samples. Each sample contained one to five conodonts, with an average of two conodonts per sample.

Insoluble residue recovered from samples collected in the Central Tennessee mining district consist mostly of carbonate rock (dolomite) and terrigenous sand, with minor amounts of quartz, fluorite, and sphalerite from samples containing mineralization. Typically, twenty five to sixty eight percent of the original rock was recovered after dissolution of samples in formic acid.

Conodont CAI

Conodont CAI range from 1 to 2.5 in conodonts recovered from samples collected in the Central Tennessee mining district. Conodonts show a wide range of CAI in individual samples collected in the district.

Conodont CAI of 2.5 were observed in conodonts recovered in samples collected between 1.5 and 31 meters from known sites of mineral deposition. Conodont CAI of 2 and 1.5 were measured in conodonts recovered in samples collected from less than 1 to 18 meters from mineralized areas, and CAI of 1 were observed in conodonts recovered from samples collected from less than 1 to 6 meters from

known sites of mineralization.

The data shows a wide lateral distribution of high CAI throughout the district. Furthermore, the highest CAI in each sample shows a preferred stratigraphic position in the Knox Dolomite (Fig. 18). In general, CAI of 2.5 occur high in the stratigraphic section. CAI of 1.5 and 2 are present stratigraphically below CAI of 2.5, and CAI of 1 occur near the bottom of the section.

Fluid Inclusion Microthermometry

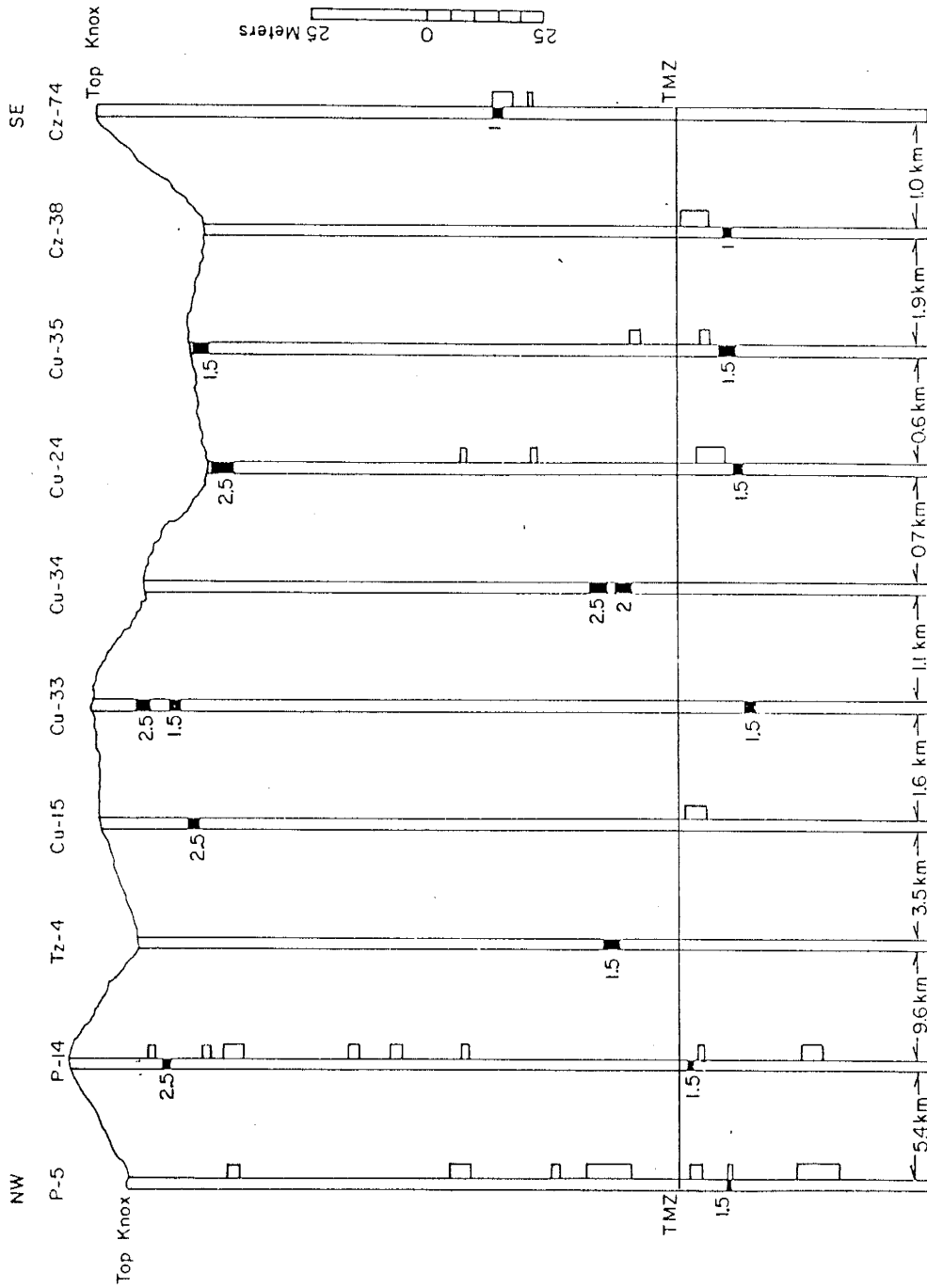
Material Studied

Fluid inclusions were examined in four samples of sphalerite and two samples of fluorite from Central Tennessee. Primary, secondary, and pseudosecondary inclusions were analyzed to determine temperatures of homogenization and melting. Most inclusions consist of the two phase liquid-vapor type. Three phase liquid-liquid-vapor pseudosecondary inclusions were observed in sample Cu-35 1109-1111. Daughter crystals were not observed in any of the inclusions. From the visual estimation chart developed by Roedder (1972), the vapor bubble in each inclusion occupies between 7 to 14% of the inclusion's total area.

Inclusions observed in sphalerite occur in localized clusters. These inclusions are elongated and commonly aligned end to end. As a result, they are difficult to

Figure 18

Lateral and stratigraphic distribution of highest conodont
CAI (■) in each sample relative to mineralization
(rectangles on right side of each core) in the Central
Tennessee mining district.



classify as either primary or secondary inclusions. Primary inclusions were differentiated from secondary inclusions by their differences in temperatures of homogenization. The size of inclusions observed in sphalerite samples is between 10 and 100 microns.

Fluorite samples contain primary inclusions which are commonly greater than 100 microns. These inclusions are randomly distributed throughout the samples. Secondary inclusions are much smaller than primary inclusions. Secondary inclusions in fluorite are elongated and aligned end to end along planes.

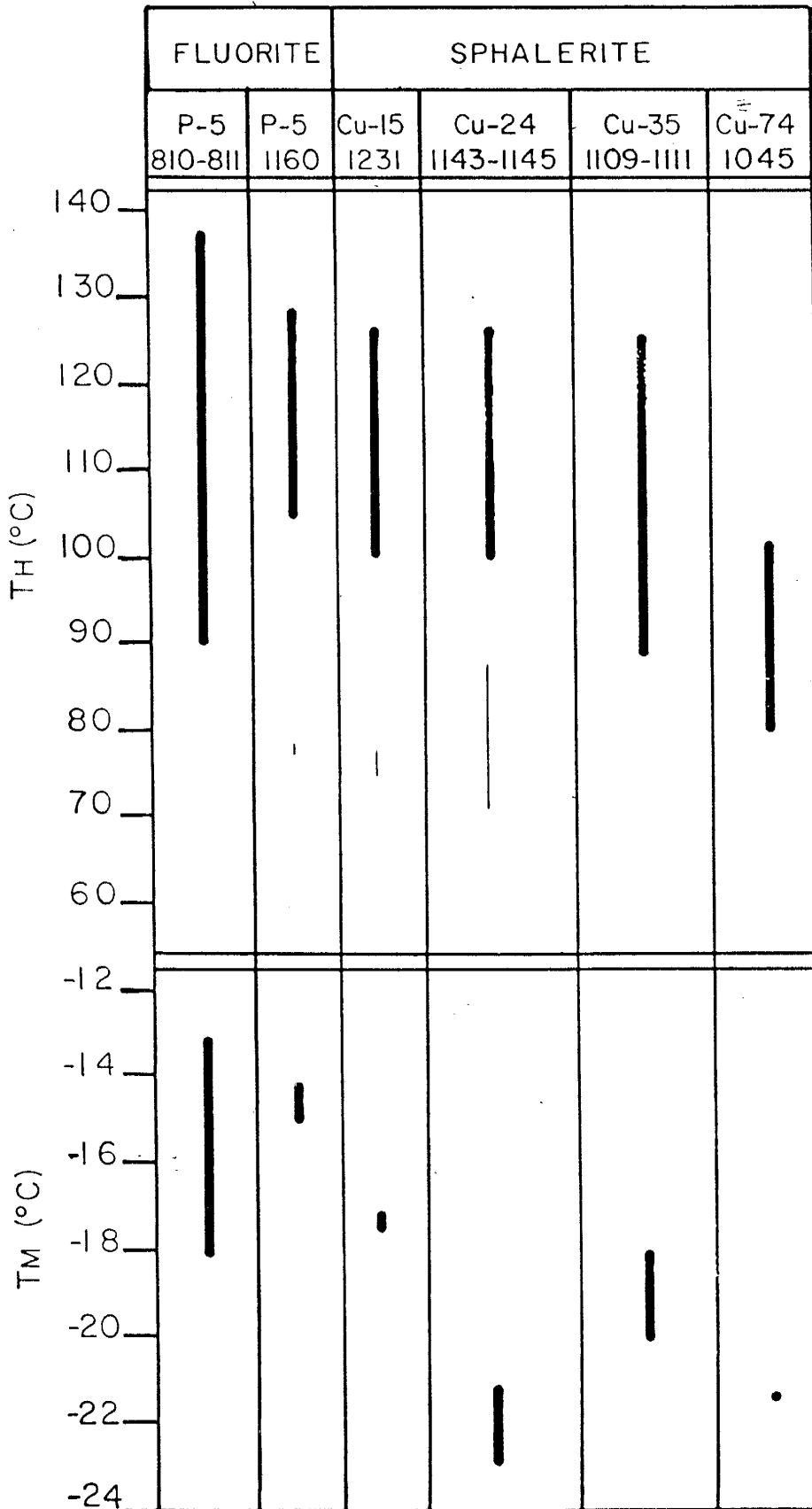
Temperature of Homogenization

Temperatures of homogenization were measured in one hundred seven inclusions. Figure 19 shows the range of fluid inclusion homogenization temperatures in individual samples.

Similar temperatures were measured in fluorite and sphalerite. They range from 80°C to 138°C. These temperatures show substantial correlation with fluid inclusion homogenization temperatures recorded in inclusions from Central Tennessee by Roedder (1971) and DeGroot (1973).

Figure 19

Range of temperatures of homogenization and melting for fluid inclusions in sphalerite and fluorite from the Central Tennessee mining district. Bold face lines represent temperatures of homogenization for primary inclusions and thin lines represent temperatures of homogenization for secondary inclusions.



Temperature of Melting

The temperature of melting was measured in twenty inclusions in sphalerite and fluorite from the Central Tennessee mining district (Fig. 19). Some temperatures of melting were lower than -21.1°C , which is the eutectic for a pure $\text{NaCl-H}_2\text{O}$ system. These low temperatures indicate that other salts, possibly CaCl_2 , are present in the system (Roedder, 1971)

Temperatures of melting for inclusions in sphalerite are between -17.7°C and -23.2°C , with the mode at -21.0°C .

The temperatures of melting for inclusions in fluorite are between -12.9°C and -18.1°C , with the mode at -15.0°C .

The temperatures of melting measured in this study are in agreement with temperatures of melting measured by Roedder (1971).

Silica Crystallite Size

The sizes of silica-crystallites were measured in eight samples of nodular chert from the Central Tennessee mining district (Table 4). Several samples contained both a light and dark fraction. These fractions were separated and the size of silica crystallite was measured two times.

The range in size of silica-crystallites is from 471A to 1109A. Temperatures calculated from these measurements are between 190°C and 263°C . Samples which were analyzed twice show discrepancies in crystallite size from between 19A and 216A. The difference in resultant temperatures is between 2°C and 24°C .

Table 4

Temperatures calculated from the size of silica-crystallites for samples of nodular chert in the Central Tennessee mining district.

SAMPLE NUMBER	SILICA CRYSTALLITE SIZE (A)	TEMPERATURE (°C)
Cu-15 1230	1109	263
Cu-15 1232	1065	259
Cu-34 1446-1449 (D)	623	212
Cu-34 1446-1449 (D)	839	236
Cu-34 1446-1449 (L)	858	237
Cu-34 1446-1449 (L)	665	217
Cu-34 1466 (L)	986	251
Cu-34 1466 (L)	1086	261
Cu-34 1466 (D)	859	239
Cu-34 1466 (D)	968	250
Cu-35 759 (L)	819	235
Cu-35 759 (L)	838	237
Cu-35 759 (D)	471	190
Cu-35 759 (D)	641	214
Cu-35 1117	766	229
Cz-38 901	719	223
Cz-38 1201	895	242

Note: D=Dark Fraction; L=Light Fraction

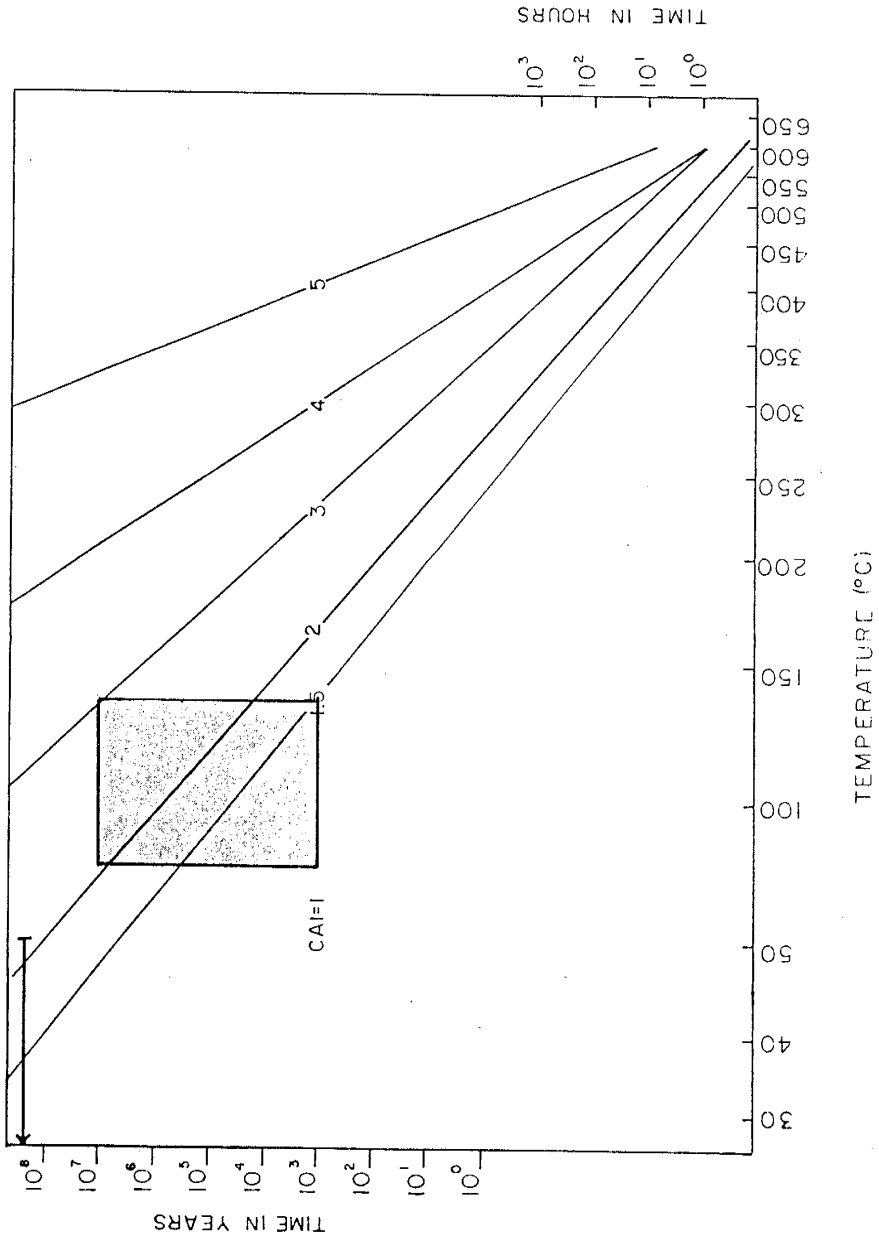
INTERPRETATION OF CENTRAL TENNESSEE

Only a crude estimate of background CAI can be made through a reconstruction of the burial history of Central Tennessee. This is due to a lack of published literature and the large number of unconformities in the area. Presently, there are 500 meters of Middle Ordovician through Mississippian rocks overlying the Knox Dolomite in Central Tennessee (Kyle, 1973; Wilson, 1949). The area may have been covered by an additional kilometer of Paleozoic strata (Wilson and Stearns, 1960; Wilson, 1948). The Mesozoic and Cenozoic Eras were intervals of subaerial exposure and denudation (Wilson, 1948). Central Tennessee was apparently covered by a minimum of 500 meters of strata and a maximum of 1.5 kilometers of strata from Lower Ordovician to the beginning of Mesozoic time (275 million years).

Temperatures less than 48°C were calculated for these depths assuming an average geothermal gradient of $32^{\circ}\text{C}/\text{km}$. Based on the published Arrhenius plot from Epstein et al. (1977), CAI of 1, 1.5, and 2 would be predicted to occur in conodonts subjected to temperatures less than 48°C for 275 million years (Fig. 20). Epstein et al. (1977, fig. 13) examined conodonts recovered from Ordovician limestones in the vicinity of the Central Tennessee mining district. They contend that CAI of 1.5 were related to temperatures associated with burial. Based on my observations I believe that CAI of 1 or 1.5 represent background CAI in the

Figure 20

Arrhenius plot of temperature versus time, showing predicted CAI associated with burial (bar with arrow) and CAI related to the deposition of hydrothermal minerals (shaded) in the Central Tennessee mining district (after Epstein et al., 1977).



Central Tennessee mining district.

The duration of mineral deposition in Central Tennessee is not presently known. Roedder (1960) set general time constraints from 1 thousand years to 10 million years for the deposition of Mississippi Valley-type deposits. Fluid inclusion homogenization temperatures determined in the present study are between 80°C and 138°C. CAI related to hydrothermal activity were estimated using these general time limits and fluid inclusion homogenization temperatures (Fig. 20). Figure 20 shows that CAI between 1.5 and 3 would be predicted to occur as a result of hydrothermal activity associated with mineral deposition.

CAI of 1.5, 2, and 2.5 are present in the Central Tennessee mining district in the Central Tennessee mining district. These CAI are present throughout the district. Therefore, I propose that CAI of 2 and 2.5 observed in the Central Tennessee mining district resulted from regional heating related to either hydrothermal fluids responsible for mineral deposition, or from hot solutions responsible for deposition of coarsely crystalline dolomite which predated ore deposition (Kyle, 1976; Harris, 1971; Hoagland, 1976). Color alteration to CAI of 1.5 may have resulted from hydrothermal activity or from temperatures related to burial.

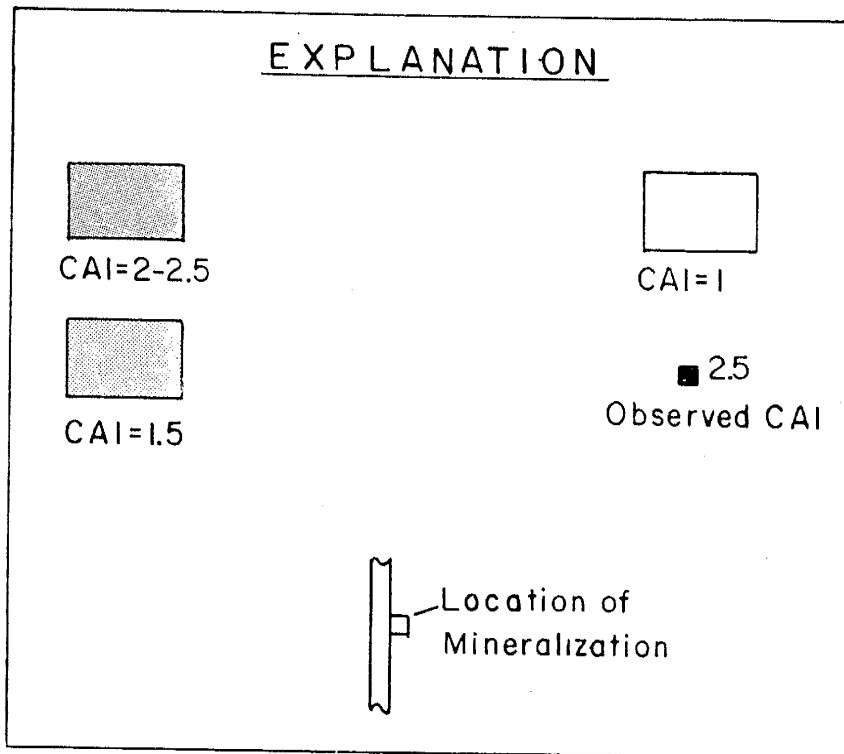
The stratified nature of CAI (Fig. 21) in Central Tennessee suggests that the hottest fluids were located near the top of the Mascot Dolomite. The location of elevated CAI with respect to the mineralization further suggests that hydrothermal fluids migrated from below towards the top of the Knox Dolomite. The geometry of dissolution cavities (Winslow and Hill, 1974) and nature of the brecciation (Kyle, 1973 and 1976) support this hypothesis.

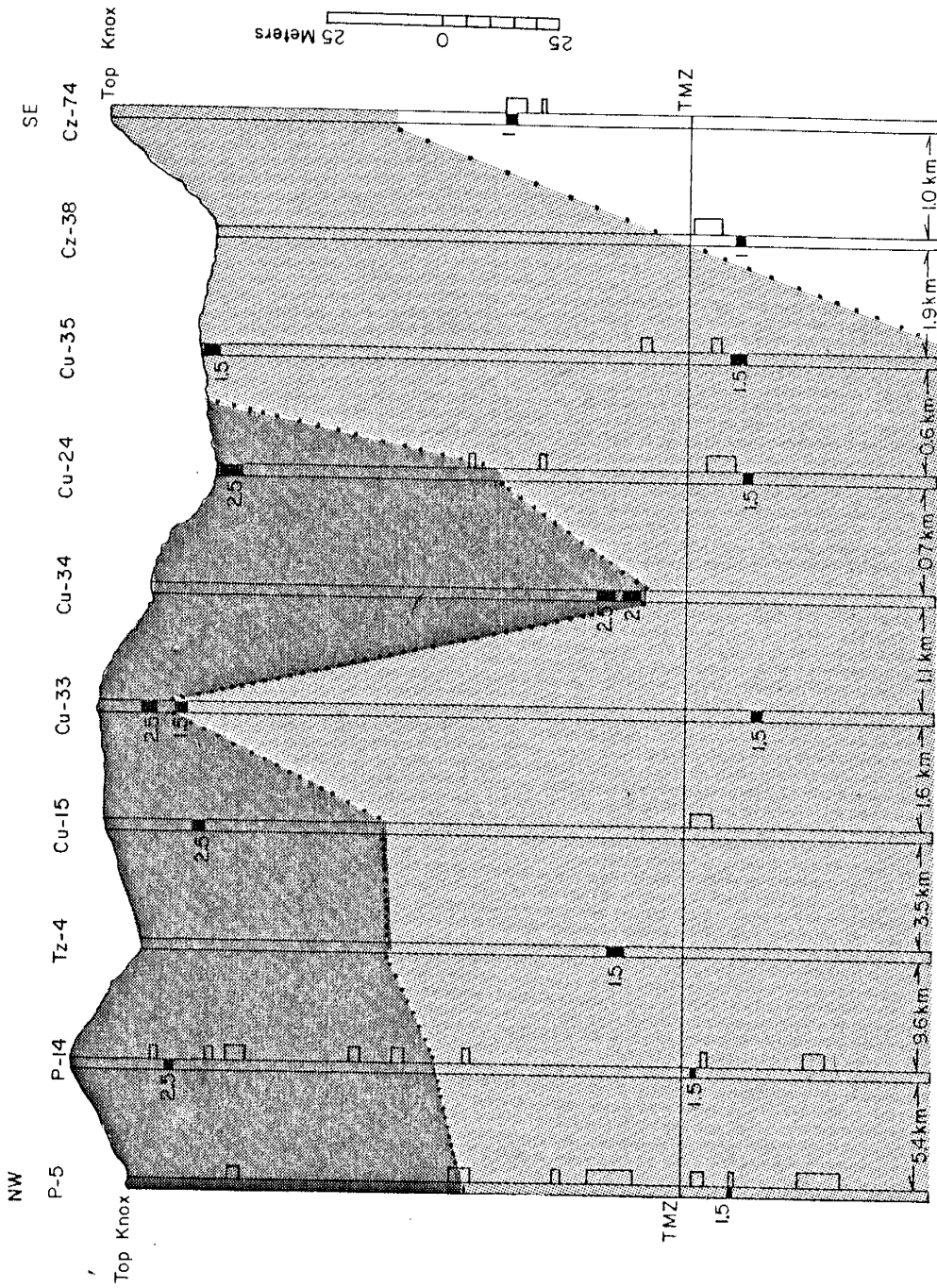
The distribution of elevated CAI in the Central Tennessee is similar to the distribution of CAI in the Hansonburg mining district. Elevated CAI in both districts are proximal to open solution channelways that were responsible for controlling the migration of hydrothermal fluids. In the Hansonburg mining district high CAI are located near northwest-trending faults associated with the mineral deposits, and in the Central Tennessee mining district CAI are associated with dissolution zones. Furthermore, elevated CAI in both districts occur stratigraphically above the mineral deposits, indicating the presence of high temperatures above the deposits.

The nature of CAI in the two districts differ in that the highest CAI at Hansonburg are localized immediately around mineral deposits, whereas high CAI in Central Tennessee mining district are regionally distributed throughout the district. These different distributions in CAI between the two deposits may be related to the

Figure 21

Conodont CAI contour profile showing proposed distribution of CAI in the Central Tennessee mining district.





availability and extent of solution channelways. In the Hansonburg mining district open channelways are limited to faults and to some extent the 6 meter thick Council Spring Limestone (Putnam and Norman, 1983). In contrast, in the Central Tennessee mining district solution channelways in carbonate rocks occur over a large lateral (10's of kilometers) and vertical (100's of meters) scale (Kyle, 1973).

CONCLUSIONS

I have shown that conodont-color is affected by hydrothermal activity associated with mineral deposition. CAI significantly higher than predicted background values were observed in each of the areas studied. These CAI correspond to temperatures of homogenization measured in hydrothermally deposited minerals.

As an exploration tool, this technique is most promising for locating deposits similar to the deposits present in the Hansonburg mining district. Progressive increases in CAI towards mineral deposits coupled with the large areal extent of these CAI can be used to define the thermal aureoles around these deposits and target potential sites of mineralization.

In the case of large-scale Mississippi Valley-Type deposits, such as the Central Tennessee mining district, this technique can be used to distinguish regional heating associated with hydrothermal activity. Therefore, this technique might be used in the initial stages of an exploration program to delineate "hot" regions affected by hydrothermal activity from "cold" regions unaffected by thermal events.

Conodont CAI may also be used to delineate regional heating trends associated with magmatic bodies, but these large-scale heating trends would prohibit delineating mineral deposits spatially or temporally related to igneous

activity. Therefore, this technique is recommended as a general reconnaissance tool to define regions affected by magmatic activity, which may be responsible for mineral deposition.

The major advantage of using conodont CAI is that this technique is simple and inexpensive. The two major deterrents of this technique are that conodont extraction and separation is relatively time consuming, and a large number of conodonts are needed to accurately determine whether an area has been affected by hydrothermal activity.

SUGGESTIONS FOR FUTURE STUDY

This study was intended to examine possible applications of conodont color alteration as a potential exploration tool for mineral deposits. As a result of this study it is apparent that more work needs to be done in these areas:

Detailed stratigraphic and lateral analysis of conodont CAI at the Hansonburg mining district to better define the thermal aureoles around mineral deposits. Detailed grid sampling and subsequent analysis of CAI should better indicate the geometry and extent of thermal activity around these deposits.

Determination of conodont CAI needs to be standardized. A study using transmitted light, uniformly sectioned conodonts, and a photometer might prove to be very instructional.

Finally additional work needs to be done determining the cause of anomalously high temperatures determined from the silica crystallite geothermometer.

REFERENCES CITED

- Abramson, B.S., 1981, The mineralizing fluids responsible for skarn and ore formation at the Continental mine, Fierro, New Mexico, in light of REE analyses and fluid inclusion studies: unpublished M.S. thesis, New Mexico Institute of Mining and Technology, 143 p.
- Allmendinger, R.J., 1975, A model for ore-genesis in the Hansonburg mining district, New Mexico: unpublished Ph.D. thesis, New Mexico Institute of Mining and Technology, 190 p.
- Barnes, C.R., Sass, D.B., and Munroe, R.A., 1973, Ultrastructure of some Ordovician conodonts: in Rhodes, F.H.T. (editor), Conodont Paleozoology: Geol. Soc. Am. Spec. Paper 141, p. 1-30.
- Beane, R.E., 1974, Barite-fluorite-galena deposits in south-central New Mexico: a product of shallow intrusions, groundwater, and epicontinental sediments: Geol. Soc. Amer. Abstracts with Programs, no. 7, p. 678-684.
- Bergstrom, S.M., 1980, Conodonts as paleo-temperature tools in Ordovician rocks of the Caledonides and adjacent areas in Scandinavia and the British Isles: Geologiska Foreningens i Stockholm Forhandlingar, v. 102, p. 377-392.
- Brasier, M.D., 1980, Appendix-reconnaissance methods: in Microfossils, p. 162-168.
- Braun, E.R., 1983, Ore controls--Middle Tennessee zinc deposit: in G Kisvarsanyi, S.K. Grant, W.P. Pratt, and J.W. Koenig (editors), International Conference on Mississippi Valley-Type Lead Zinc Deposits, Univ. of Missouri-Rolla, Rolla, Mo., p.349-359.
- Cathles, L.M., 1977, An analysis of the cooling of intrusives by groundwater convection which includes boiling: Econ. Geol., v. 72, p. 804-826.
- Cathles, L.M., 1981, Fluid flow and genesis of ore deposits: in B.J. Skinner (editor), Econ. Geol. 75th Anniv. Vol., p. 424-457.

- Chapin, C.E., 1979, Evolution of the Rio Grande Rift-a summary: in R.E. Riecker (editor), Tectonics and Magmatism, Amer. Geophys. Union, Washington, D.C.
- DeGroot, J.H., Jr., 1973, Determination of temperatures of fluorite formation by fluid inclusion thermometry, Central Tennessee (abs.): Geol. Soc. Amer., Southeastern Section Annual Meeting, Abstracts with Programs, v. 5, no. 5, p. 394.
- Duba, D., and Williams-Jones, A.E., 1983, The application of illite crystallinity, organic matter reflectance, and isotopic techniques to mineral exploration: A case study in southwestern Gaspe', Quebec: Econ. Geol., v. 78, p. 1350-1363.
- Ellison, S., 1944, The composition of conodonts: Jour. Paleontology, v. 18, p. 133-140.
- Epstein, A.G., Epstein, J.B., and Harris, L.D., 1977, Conodont color alteration-an index to organic metamorphism: U.S. Geol. Surv. Prof. Paper 995, 27 p.
- Ewing, T.E., 1979, Lead isotope data from the mineral deposits of southern New Mexico: a reinterpretation: Econ. Geol., v. 74, p. 678-684.
- Folk, R.L., 1959, Practical petrographic classification of limestones: Am. Assoc. Petrol. Geologists Bull., v. 43, p. 1-38.
- Foster, N.H., 1966, Stratigraphic leak: Am. Assoc. Petrol. Geologists Bull., v. 50, p. 2604-2606.
- Gray, D.R., 1981, Compound tectonic fabrics in singly folded rocks from southwest Virginia, U.S.A.: Tectonophysics, v. 78, p. 229-248.
- Harris, L.D., 1971, A Lower Paleozoic paleoaquifer--the Kingsport Formation and Mascot Dolomite of Tennessee and Southwest Virginia: Econ. Geol., v. 66, p. 735-743.
- Harris, L.D., Harris, A.G., DeWitt, W. and Bayer, K.C., 1981, Evaluation of the southern Eastern overthrust belt beneath Blue Ridge-Piedmont thrust: Am. Assoc. Petrol. Geologists Bull., v. 65, p. 2497-2505.

- Harrower, R.D., 1981, Stable oxygen isotope and crystallite size analysis of Alaskan cherts: A possible exploration tool for submarine exhalative deposits: unpublished M.S. thesis, New Mexico Institute of Mining and Technology, 55 p.
- Hernon, R.M., and Jones, W.R., 1967, Ore deposits in the Central mining district, Grant County, New Mexico: in John Ridge (editor), Ore Deposits of the United States, A.I.M.E., v. 2, p. 1211-1237.
- Hoagland, A.D., 1976, Appalachian zinc-lead deposits: in Wolf, K.E. (editor), Handbook of strata-bound and stratiform ore deposits, v. 1, p. 495-533.
- Holland, R.A.G., Bray, C.J., and Spooner, E.T.C., 1978, A method for preparing doubly polished thin sections suitable for microthermometric examination of fluid inclusions: Mineral Mag., v. 42, p. 407-408.
- Ilchik, R.P., 1984, Hydrothermal maturation of organic matter at the Alligator Ridge gold deposits, Nevada: in Geol. Soc. Amer. Abstracts with Programs, v. 16, no. 6, p. 548.
- Jaeger, J.C., 1957, The temperature in the neighborhood of a cooling intrusive sheet: Am. Jour. Sci., v. 255, p. 306-318.
- Jaeger, J.C., 1959, Temperature outside a cooling intrusive sheet: Am. Jour. Sci., v. 257, p. 44-54.
- Jones, W.R., Hernon, R.M., and Moore, S.L., 1967, General geology of the Santa Rita quadrangle, Grant County, New Mexico: U.S. Geol. Survey Prof. Paper 555, 144 p.
- Koch, G.S., Jr., and Link, R.F., 1970, Statistical analysis of geological data: John Wiley and Sons Inc., 375p.
- Kottowski, F.E., 1953, Geology and ore deposits of a part of the Hansonburg mining district, Socorro County, New Mexico: New Mexico Bureau of Mines and Mineral Resources Cir. 23, 9 p.
- Kyle, J.R., 1973, Preliminary investigation of brecciation, alteration, and mineralization in the upper Knox Group of Smith and Trousdale Counties, Tennessee: unpublished M.S. thesis, University of Tennessee, 93 p.

- Kyle, J.R., 1976, Brecciation, alteration, and mineralization in the Central Tennessee zinc district: *Econ. Geol.*, v. 71, p. 892-903.
- Legall, F.D., Barnes, C.R., and MacQueen, R.W., 1981, Thermal maturation, burial history, and hot-spot development, Paleozoic strata of southern Ontario-Quebec, from conodont and acritarch color alteration studies: *Bull. Can. Petrol. Geol.*, v. 29, p. 492-539.
- Lovering, T.S., 1935, Theory of heat conduction applied to geological problems: *Geol. Soc. Am. Bull.*, v. 46, p. 69-93.
- Mayr, U., Uyeno, T.T., and Barnes, C.R., 1978, Subsurface stratigraphy, conodont zonation, and organic metamorphism of the Lower Paleozoic succession, Bjerne Peninsula, Ellesmere Island, District of Franklin: in *Current Research, Part A, Geol. Survey Can. Paper 78-1A*, p. 393-398.
- Norman, D.I., Ting, W., Putnam, B.R., III, and Smith, R.W., 1985, Mineralization of the Hansonburg Mississippi Valley-type deposit, New Mexico: insight from composition of gases in fluid inclusions: *Canadian Mineralogist*, v. 23, p. 353-368.
- Nowlan, G.S., 1983, Biostratigraphic, paleogeographic, and tectonic implications of Late Ordovician conodonts from the Grog Brook Group, northwestern New Brunswick: *Can. Jour. Earth Sci.*, v. 20, p. 651-671.
- Perry, W.J., Harris, A.G., and Harris, L.D., 1979, Conodont-based reinterpretation of Bane Dome-structural reevaluation of Allegheny frontal zone: *Am. Assoc. Petrol. Geologists Bull.*, v. 63, p. 647-654.
- Perry, W.J., Wardlaw, B.R., Bostick, N.H., and Maughan, E.K., 1983, Structure, burial history, and petroleum potential of frontal thrust belt and adjacent foreland, southwest Montana: *Am. Assoc. Petrol. Geologists Bull.*, v. 67, p. 725-743.

- Putnam, B.R., III, and Norman, D.I., 1983, Genetic model for Hansonburg Mississippi Valley-type mineralization in New Mexico. Based on fluid inclusion studies in paleotectonic interpretations: in G. Kisvarsanyi, S.K. Grant, W.P. Pratt, and J.W. Koenig (editors), International Conference on Mississippi Valley-Type Lead-Zinc Deposits, Univ. of Missouri-Rolla, Rolla, Mo.
- Putnam, B.R., III, 1980, Fluid inclusion and microchemical analysis of the Hansonburg Mississippi Valley-Type ore deposits in Central New Mexico: unpublished M.S. thesis, New Mexico Institute of Mining and Technology, 126 p.
- Reiter, M., Edwards, C.L., Hartman, H., and Weidman, C., 1975, Terrestrial heat flow along the Rio Grande Rift, New Mexico and southern Colorado: Geol. Soc. Amer. Bull., v. 86, p. 811-818.
- Reiter, M., and Tovar, J.C., 1982, Estimates of terrestrial heat flow in northern Chihuahua, Mexico based on petroleum bottom-hole temperatures: Geol. Soc. Am. Bull., v. 93, p. 613-624.
- Renault, J., 1980, Application of crystallite size variation in cherts to petroleum exploration, New Mexico Energy Institute at New Mexico Institute of Mining and Technology, Final Report for Grant No. 78-3315, 22 p.
- Roedder, E., 1960, Fluid inclusions as samples of ore-forming fluids: International Geol. Conference, 21st, Copenhagen 1960, p. 218-229.
- Roedder, E., 1971, Fluid-inclusion evidence on the environment of formation of mineral deposits of the southern Appalachian Valley: Econ. Geol., v. 66, p. 777-791.
- Roedder, E., 1984, Fluid Inclusions: in Reviews in Mineralogy, v. 12, 644p.
- Roedder, E., Heyl, A.V., Creel, J.P., 1968, Environment of ore deposition at the Mex-Tex deposits, Hansonburg district, New Mexico, from studies of fluid inclusions: Econ. Geol., v. 63, p. 336-348.

- Sando, W.J., Sandberg, C.A., and Gutschick, R.C., 1981, Stratigraphic and economic significance of Mississippian sequence at North Georgetown Canyon, Idaho: Am. Assoc. Petrol. Geologists Bull., v. 65, p. 1433-1443.
- Spung, J.H., and Groshong, R.H., 1981, Deformation mechanisms and strain history of a minor fold from the Appalachian Valley and Ridge Province: Tectonophysics, v. 72, p. 323-342.
- Swanberg, C.A., 1980, Geothermal resources of New Mexico: N.M. Energy Institute at N.M.S.U., 1 map, scale 1:500,000.
- Thompson, M.L., 1942, Pennsylvanian systems in New Mexico: N.M. Bur. Mines Bull. 17, 92p.
- Wardlaw, B.R., and Collinson, J.W., 1978, Stratigraphic relations of Park City Group (Permian) in eastern Nevada and western Utah: Am. Assoc. Petrol. Geologists Bull., v. 62, p. 1171-1184.
- Wardlaw, B.R., and Harris, A.G., 1984, Conodont-based thermal maturation of Paleozoic rocks in Arizona: Am. Assoc. Petrol. Geologists Bull., v. 68, p. 1101-1106.
- Wilpolt, R.H., and Wanek, A.A., 1951, Geology of the region from Socorro and San Antonio east to Chupadera Mesa, Socorro County, New Mexico: U.S. Geol. Survey Oil and Gas Prelim. Map 121.
- Wilson, C.W., Jr., 1948, Geology of Nashville Tennessee: Tenn. Div. Geol. Bull. 53, 172p.
- Wilson, C.W., Jr., 1949, Pre-Chattanooga stratigraphy in Central Tennessee: Tenn. Div. Geol. Bull. 56, 405p.
- Wilson, C.W., Jr., and Stearns, R.G., 1960, Pennsylvanian marine cyclothems in Tennessee: Geol. Soc. Am. Bull., v. 71, p. 1451-1466.
- Winslow, K.R., and Hill, W.T., 1973, The Elmwood project: Mining Congress Jour., v. 59, no. 3, p. 19-24.

APPENDIX I

CONODONT COLOR ALTERATION

Conodont color alteration data are reported for conodonts from the Hansonburg mining district (Part A), and the Continental mine (Part B), Central Tennessee mining district (Part C) Stratigraphic units sampled, distance from possible heat sources, amount of carbonate rock digested in formic acid, conodont morphology, conodont volume and color alteration index is reported for each conodont studied.

The following abbreviations were used:

n/a= not applicable, either because conodonts were not recovered from samples or because unit was not sampled over specified interval (i.e. stratigraphic or areal).

SP= scaphate pectinoform

CP= carminate pectinoform

AP= angulate pectinoform

C= coniform

fr= fragmented specimen

(102)

PART A
HANSONBURG MINING DISTRICT

APPENDIX I

CONODONT COLOR ALTERATION INDICES

Hansonburg Mining District

Sample Number	Stratigraphic Unit Sampled	Distance From Mineralization Area ¹ Strat (Meters)	Amount Rock Dissolved (Kilograms)	Gross Morphology	Volume Conodont ² (x10 ⁻³ mm ³)	CAI
MT-1	Council Spring	0.3	1	n/a	n/a	n/a
MT-2	Council Spring	0.6	.5	SP	12.109	2.5
MT-2	Council Spring	0.6	.5	AP	.750	3
MT-3	Council Spring	1.2	.5	SP	7.813	3
MT-3	Council Spring	1.2	.5	SP	8.438	2
MT-4	Council Spring	1.8	1	SP	55.000	3
MT-4	Council Spring	1.8	1	SP	54.688	3
MT-4	Council Spring	1.8	1	fr	n/a	1.5
MT-4	Council Spring	1.8	1	SP	63.281	3
MT-4	Council Spring	1.8	1	SP	194.063	3
MT-4	Council Spring	1.8	1	SP	92.813	3
MT-5	Burrego Fm.	4.5	.5	SP	8.438	3
MT-6	Burrego Fm.	7.6	1	SP	1.406	1.5
MT-6	Burrego Fm.	7.6	1	SP	1.125	2
MT-7	Story Fm.	24.2	1	SP	6.875	3

Sample Number	Stratigraphic Unit Sampled	Distance From Mineralization Area ¹ Strat (Meters)	Amount Rock Dissolved (Kilograms)	Gross Morphology	Volume Conodonts (x10 ⁻³ mm ³)	CAI
MT-8	Story Fm.	36.4 30.3	1	n/a	n/a	n/a
MT-9	Bolander Gp.	53.0 45.5	1	SP	3.750	1.5
MT-9	Bolander Gp.	53.0 45.5	1	fr	fr	1.5
MT-10	Bolander Gp.	48.5 42.4	1	n/a	n/a	n/a
MT-11	Coane Fm.	37.9 33.3	1	SP	.750	2
MT-12	Adobe Fm.	18.2 13.6	1	n/a	n/a	n/a
MT-13	Adobe Fm.	12.1 9.1	1	SP	126.000	3
MT-14	Council Spring	310.6 n/a	1	CP	.938	1
MT-14	Council Spring	310.6 n/a	1	AP	1.688	1.5
MT-14	Council Spring	310.6 n/a	1	SP	1.687	1
MT-15	Council Spring	60.6 n/a	.5	AP	2.078	2.5
MT-16	Council Spring	250.0 n/a	.5	CP	1.875	1
MT-16	Council Spring	250.0 n/a	.5	CP	1.055	1
MT-16	Council Spring	250.0 n/a	.5	CP	.688	1
MT-16	Council Spring	250.0 n/a	.5	SP	1.406	1
MT-17	Council Spring	303.0 n/a	.5	CP	1.699	1
MT-18	Moya Fm.	818.6 n/a	.5	SP	2.109	1.5
MT-19	Moya Fm.	855.8 n/a	.5	SP	8.125	1

Sample Number	Stratigraphic Unit Sampled	Distance From Mineralization Areal Strat (Meters)	Amount Rock Dissolved (Kilograms)	Gross Morphology	Volume Conodont ³ ($\times 10^{-3} \text{mm}^3$)	CAI
MT-20	Moya Fm.	227.3	.5	SP	3.375	1.5
MT-20	Moya Fm.	227.3	.5	SP	4.250	1
MT-20	Moya Fm.	227.3	.5	SP	1.406	1
MT-21	Council Spring	340.9	.5	SP	10.938	1.5
MT-22	Burrego Fm.	340.9	1	n/a	n/a	n/a
MT-23	Council Spring	762.8	.5	fr	fr	1.5
MT-24	Burrego Fm.	762.8	1	n/a	n/a	n/a
MT-26	Bolander Gp.	75.8	1	SP	10.719	2
MT-26	Bolander Gp.	75.8	1	AP	3.125	2
MT-27	Bolander Gp.	106.1	1	fr	fr	1.5
C-1	Council Spring	3.0	1	n/a	n/a	n/a
C-2	Burrego Fm.	4.5	.5	fr	fr	3
C-3	Burrego Fm.	12.1	.5	SP	13.672	2
C-4	Burrego Fm.	21.2	1	n/a	n/a	n/a
C-5	Story Fm.	24.2	.5	AP	4.688	2.5
C-5	Story Fm.	24.2	.5	AP	4.375	2.5
C-5	Story Fm.	24.2	.5	SP	7.000	1
C-6	Story Fm.	30.3	.5	CP	2.500	1.5

Sample Number	Stratigraphic Unit Sampled	Distance From Mineralization Areal Strat (Meters)	Amount Rock Dissolved (Kilograms)	Gross Morphology	Volume Conodont (x10 ⁻³ mm ³)	CAI
C-7	Del Cuerto Fm.	40.9	.5	AP	15.313	3
C-7	Del Cuerto Fm.	40.9	.5	AP	6.250	1
C-8	Del Cuerto Fm.	54.5	.5	SP	15.625	2
C-8	Del Cuerto Fm.	54.5	.5	SP	11.250	2.5
C-8	Del Cuerto Fm.	54.5	.5	fr	fr	2.5
C-8	Del Cuerto Fm.	54.5	.5	fr	fr	3
ET-1	Moya Fm.	90.0	.5	SP	6.563	2
ET-2	Moya Fm.	212.1	.5	fr	fr	2
ET-3	Moya Fm.	303.0	.5	SP	15.898	1.5
ET-3	Moya Fm.	303.0	.5	fr	fr	1.5
ET-4	Moya Fm.	386.4	.5	AP	.328	1
ET-4	Moya Fm.	386.4	.5	AP	.375	1
ET-4	Moya Fm.	386.4	.5	SP	2.250	2
ET-4	Moya Fm.	386.4	.5	SP	2.250	2
ET-5	Moya Fm.	454.5	.5	AP	.438	1
ET-5	Moya Fm.	454.5	.5	AP	.106	1
ET-5	Moya Fm.	454.5	.5	SP	.688	1
ET-5	Moya Fm.	454.5	.5	SP	.305	1
ET-6	Moya Fm.	524.3	.5	AP	2.125	1
ET-6	Moya Fm.	524.3	.5	SP	.938	1
ET-6	Moya Fm.	524.3	.5	fr	fr	1
ET-7	Moya Fm.	594.0	.5	n/a	n/a	n/a

Sample Number	Stratigraphic Unit Sampled	Distance From Mineralization Area ¹ Strat (Meters)	Amount Rock Dissolved (Kilograms)	Gross Morphology	Volume Conodont ($\times 10^{-3} \text{mm}^3$)	CAI
ET-8	Moya Fm.	665.5	.5	SP	3.984	1
ET-8	Moya Fm.	665.5	.5	SP	1.594	1
ET-8	Moya Fm.	665.5	.5	SP	6.563	1
ET-8	Moya Fm.	665.5	.5	SP	4.000	1
RF-1	Story Fm.	25.8	1	AP	2.250	2.5
RF-2	Del Cuerto Fm.	33.3	1	n/a	n/a	n/a
RF-3	Moya Fm.	72.7	1	n/a	n/a	n/a
RF-4	Burrego Fm.	15.2	1.5	CP	7.031	2
RF-4	Burrego Fm.	15.2	1.5	SP	5.859	3
RF-4	Burrego Fm.	15.2	1.5	fr	fr	3
RF-4	Burrego Fm.	15.2	1.5	CP	2.031	3
RF-4	Burrego Fm.	15.2	1.5	CP	2.625	3
RF-4	Burrego Fm.	15.2	1.5	CP	.938	3
RF-5	Adobe Fm.	12.1	2	fr	fr	2.5
RF-6	Adobe Fm.	15.2	1.5	n/a	n/a	n/a
RF-7	Coane Fm.	24.2	2	fr	fr	3
RF-8	Council Spring	138.5	1	SP	.844	1.5
RF-9	Council Spring	356.1	1	SP	1.063	1.5
RF-10	Council Spring	744.2	.5	AP	6.563	2.5
RF-11	Council Spring	3.0	.5	SP	2.109	1.5

Sample Number	Stratigraphic Unit Sampled	Distance From Mineralization Areal Strat (Meters)	Amount Rock Dissolved (Kilograms)	Gross Morphology	Volume Conodonts ($\times 10^{-3} \text{mm}^3$)	CAI
RF-11	Council Spring	3.0	.5	SP	2.813	3
RF-11	Council Spring	3.0	.5	SP	11.719	3
RF-11	Council Spring	3.0	.5	SP	4.750	2
RF-11	Council Spring	3.0	.5	CP	.625	2.5
RF-11	Council Spring	3.0	.5	SP	5.500	1.5
RF-11	Council Spring	3.0	.5	SP	4.890	1
RF-11	Council Spring	3.0	.5	SP	22.969	1.5
RF-11	Council Spring	3.0	.5	SP	26.563	3
RF-11	Council Spring	3.0	.5	fr	fr	3
RF-11	Council Spring	3.0	.5	SP	6.563	1.5
RF-11	Council Spring	3.0	.5	SP	7.188	1.5
RF-12	Burrego Fm.	22.7	1	n/a	n/a	n/a
RF-13	Burrego Fm.	22.7	1	SP	52.500	3
RF-13	Burrego Fm.	22.7	1	CP	1.063	1.5
RF-13	Burrego Fm.	22.7	1	fr	fr	3
RF-13	Burrego Fm.	22.7	1	SP	3.984	2.5
RF-13	Burrego Fm.	22.7	1	SP	15.898	3
RF-14	Del Cuerto Fm.	295.5	1	SP	2.813	1
RF-14	Del Cuerto Fm.	295.5	1	SP	2.531	1
RF-14	Del Cuerto Fm.	295.5	1	CP	1.875	1.5
RF-15	Del Cuerto Fm.	219.7	.5	SP	3.375	1.5
RF-15	Del Cuerto Fm.	219.7	.5	AP	2.625	1.5
RF-15	Del Cuerto Fm.	219.7	.5	fr	fr	1.5
RF-16	Del Cuerto Fm.	356.1	.5	fr	fr	1.5
RF-16	Del Cuerto Fm.	356.1	.5	SP	2.109	1
RF-16	Del Cuerto Fm.	356.1	.5	SP	2.109	1

Sample Number	Stratigraphic Unit Sampled	Distance From Mineralization Areal Strat (Meters)	Amount Rock Dissolved (kilograms)	Gross Morphology	Volume Comogonit ($\times 10^{-3} \text{mm}^3$)	CAI
RF-17	Burrego Fm.	174.2	1	SP	4.000	1
CS-1	Council Spring	372.8	1	SP	2.813	1.5
CS-2	Council Spring	539.5	1	SP	1.875	1
BS-1	Moya Fm.	1247.0	.5	n/a	n/a	n/a
BS-2	Moya Fm.	1340.0	.5	SP	1.500	1
BS-3	Moya Fm.	1488.0	.5	CP	5.000	1
BS-3	Moya Fm.	1488.0	.5	fr	fr	1
BS-4	Moya Fm.	1674.0	.5	n/a	n/a	n/a
BS-5	Moya Fm.	1879.0	.5	CP	3.516	1
BS-6	Moya Fm.	2065.0	.5	n/a	n/a	n/a
BS-7	Moya Fm.	2251.0	.5	fr	fr	1
BS-8	Moya Fm.	2400.0	.5	SP	2.813	1
HH-1	Council Spring	465.0	1	SP	7.188	1.5
HH-1	Council Spring	465.0	1	fr	fr	1.5
HH-2	Council Spring	278.8	1.5	n/a	n/a	n/a
HH-3	Council Spring	1.0	.5	SP	14.625	1.5
HH-3	Council Spring	1.0	.5	CP	.375	1
HH-3	Council Spring	1.0	.5	CP	.313	1

Sample Number	Stratigraphic Unit Sampled	Distance From Mineralization Area Strat (Meters)	Amount Rock Dissolved (Kilograms)	Gross Morphology	Volume Conodont ($\times 10^{-3} \text{mm}^3$)	CAI
HH-4	Council Spring	15.2	1	n/a	n/a	n/a
HH-5	Council Spring	45.5	1	n/a	n/a	n/a
HH-6	Council Spring	409.0	1	n/a	n/a	n/a
HH-7	Council Spring	427.9	1	n/a	n/a	n/a

(111)

PART B
CONTINENTAL MINE

Continental Mine

Sample Number	Stratigraphic Unit Sampled	Areal Distance From Mine Stock	Amount Rock Dissolved (Kilograms)	Gross Morphology	Volume Conodont ($\times 10^{-3} \text{mm}^3$)	CAI
MLV-1	Lake Valley	3000	.5	CP	3.025	5
MLV-2	Lake Valley	2385	1	n/a	n/a	n/a
MLV-3	Lake Valley	2385	1	n/a	n/a	n/a
MLV-4	Lake Valley	2385	1	n/a	n/a	n/a
MLV-5	Lake Valley	2215	1	CP	3.500	5
MLV-5	Lake Valley	2215	1	CP	3.750	5
MLV-5	Lake Valley	2215	1	CP	4.250	5
MLV-5	Lake Valley	2215	1	CP	3.750	5
MLV-6	Lake Valley	1092	1	CP	3.000	5
MLV-7	Lake Valley	697	.5	n/a	n/a	n/a
MLV-8	Lake Valley	1538	.5	CP	2.344	6
MLV-8	Lake Valley	1538	.5	CP	2.625	6
MLV-9	Lake Valley	6555	1	n/a	n/a	n/a
LVL-40	Lake Valley	8245	.5	CP	4.688	3
LVL-40	Lake Valley	8245	.5	CP	7.031	3
LVL-40	Lake Valley	8245	.5	CP	4.687	3
LVL-40	Lake Valley	8245	.5	CP	3.750	3
LVL-40	Lake Valley	8245	.5	CP	5.313	3

Sample Number	Stratigraphic Unit Sampled	Area Distance From Mine Stock	Amount Rock Dissolved (Kilograms)	Gross Morphology	Volume Conodont (x10 ⁻³ mm ³)	CAI
Po-1	Oswaldo Fm	3755	.5	CP	37.500	4
Po-2	Oswaldo Fm	3015	1	n/a	n/a	n/a
Po-4	Oswaldo Fm	3061	.5	CP	23.438	3
Po-4	Oswaldo Fm	3061	.5	P	fr	3
Po-5	Oswaldo Fm	5815	.5	CP	4.219	4
Po-5	Oswaldo Fm	5815	.5	CP	14.875	4
Po-5	Oswaldo Fm	5815	.5	CP	2.813	4
Po-5	Oswaldo Fm	5815	.5	CP	10.000	4
Po-5	Oswaldo Fm	5815	.5	CP	2.813	4
Po-5	Oswaldo Fm	5815	.5	CP	2.344	4
Po-5	Oswaldo Fm	5815	.5	CP	4.688	4
Po-5	Oswaldo Fm	5815	.5	CP	4.266	4
Po-5	Oswaldo Fm	5815	.5	CP	4.500	4
Po-6	Oswaldo Fm	5754	.5	CP	4.250	4
Po-6	Oswaldo Fm	5754	.5	CP	5.000	4
Po-7	Oswaldo Fm	3739	.5	CP	3.047	4
Po-7	Oswaldo Fm	3739	.5	CP	28.875	5
Po-8	Oswaldo Fm	3385	.5	CP	16.250	4
Po-8	Oswaldo Fm	3385	.5	CP	28.125	4
Po-9	Oswaldo Fm	3445	.5	n/a	n/a	n/a
MP-1	Miss-Penn	0	1.5	n/a	n/a	n/a

Sample Number	Stratigraphic Unit Sampled	Area Distance From Mine Stock	Amount Rock Dissolved (Kilograms)	Gross Morphology	Volume Conodonts ($\times 10^{-3}$ mm ³)	CAI
MP-3	Miss-Penn	0	1.5	n/a	n/a	n/a
Ps-1	Syrena Fm	2523	1	n/a	n/a	n/a
Om-1	Montoya Fm	0	1	n/a	n/a	n/a

PART C
CENTRAL TENNESSEE MINING DISTRICT

Sample Number	Stratigraphic Unit Sampled	Trace	>1% Grade (Meters)	Distance From Frac	Brec (Kilograms)	Amount Rock Dissolved	Gross Morphology ($\times 10^{-3} \text{mm}^3$)	Volume Conodont	CAI
P-5									
756-758	Upper Mascot	16.0	122.0	0.5	0	1	n/a	n/a	n/a
810-811	Upper Mascot	1.5	106.0	0	15.0	.5	n/a	n/a	n/a
1160	Middle Mascot	0.5	0.5	0	1.5	.5	C	ff	1
1170-1172	Middle Mascot	4.0	3.0	3.0	0	2	n/a	n/a	n/a
P-14									
798-799.5	Upper Mascot	1.5	31.0	0.5	7.0	.5	C	51.563	2.5
798-799.5	Upper Mascot	1.5	31.0	0.5	7.0	.5	C	15.469	1.5
798-799.5	Upper Mascot	1.5	31.0	0.5	7.0	.5	C	ff	1
1160-1161	Middle Mascot	1.0	20.0	0	5.0	1	C	7.250	1.5
Tz-4									
844-846	Upper Mascot	20.0	n/a	5.0	1.0	1	n/a	n/a	n/a
1135-1138	Middle Mascot	18.0	n/a	0	18.0	.5	C	1.125	1.5
1326	Middle Mascot	0.5	n/a	0	6.0	1	n/a	n/a	n/a
Cu-15									
880-882	Upper Mascot	1.5	104.0	2.0	0	1.5	C	23.438	2.5
1230-1232	Middle Mascot	0.5	2.0	0	2.5	1.5	n/a	n/a	n/a
Cu-33									
981-983	Upper Mascot	8.0	n/a	3.0	1.5	.5	C	8.750	2.5
1000-1002	Upper Mascot	2.0	n/a	3.0	1.5	1.5	C	2.750	1.5
1000-1002	Upper Mascot	2.0	n/a	3.0	1.5	1.5	C	5.469	1.5
1356-1358	Middle Mascot	0.5	n/a	0	0.5	2	C	6.563	1.5

Sample Number	Stratigraphic Unit Sampled	Trace	>1% Grade (Meters)	Distance From Frac	Brec (Kilograms)	Amount Rock Dissolved	Gross Morphology ($\times 10^{-3} \text{mm}^3$)	Volume Conodont	CAI
Cu-34									
1192-1195	Upper Mascot	5.0	n/a	1.0	0.5	2	n/a	n/a	n/a
1446-1449	Middle Mascot	5.0	n/a	0.5	71.5	1.5	C	7.500	2.5
1446-1449	Middle Mascot	5.0	n/a	0.5	71.5	1.5	C	50.265	2.5
1446-1449	Middle Mascot	5.0	n/a	0.5	71.5	1.5	C	2.813	1.5
1465-1468	Middle Mascot	0.5	n/a	0	66.5	1.5	C	7.000	2
1465-1468	Middle Mascot	0.5	n/a	0	66.5	1.5	C	2.734	1.5
1465-1468	Middle Mascot	0.5	n/a	0	66.5	1.5	C	3.281	1.5
1465-1468	Middle Mascot	0.5	n/a	0	66.5	1.5	C	6.328	1.5
1465-1468	Middle Mascot	0.5	n/a	0	66.5	1.5	C	3.125	1.5
Cu-24									
790-794	Upper Mascot	30.0	49.0	3.5	0	.5	C	21.094	2.5
1143-1145	Middle Mascot	0.5	0.5	1.0	0	.5	n/a	n/a	n/a
1146-1149	Middle Mascot	0.5	0.5	1.5	0	.5	C	22.500	1.5
Cu-35									
757-760	Upper Mascot	3.5	63.0	0.5	1.5	1.5	C	9.375	1.5
1109-1111	Middle Mascot	0.5	0.5	0.5	0.5	.5	n/a	n/a	n/a
1117-1120	Middle Mascot	2.0	2.0	0.5	1.5	.5	C	3.500	1.5
1117-1120	Middle Mascot	2.0	2.0	0.5	1.5	.5	C	2.500	1.5
Cz-38									
900-902	Upper Mascot	46.0	93.0	0.5	2.5	1.5	n/a	n/a	n/a
1201-1202	Middle Mascot	0.5	0.5	0.5	0	1	n/a	n/a	n/a
1203-1205	Middle Mascot	0.5	0.5	2.5	0	1.5	n/a	n/a	n/a
1212	Middle Mascot	0.5	0.5	5.5	0	.5	n/a	n/a	n/a
1236-1238	Middle Mascot	6.0	7.5	0.5	2.0	.5	C	fr	1

Sample Number	Stratigraphic Unit Sampled	Trace	>1% Grade (Meters)	Distance From Frac	Brec (Kilograms)	Amount Rock Dissolved	Gross Morphology ($\times 10^{-3} \text{mm}^3$)	Volume Conodont	CAI
Cz-74									
815-817	Upper Mascot	27.5	63.5	0.5	6.0	1	n/a	n/a	n/a
1044-1046	Middle Mascot	0.5	0.5	0	6.5	1	C	2.578	1
1182-1185	Middle Mascot	15.5	15.5	1.5	4.5	.5	n/a	n/a	n/a

APPENDIX II
FLUID INCLUSION DATA

Fluid inclusion data are reported for each deposit studied. The type of material studied, type of inclusion studied, heating and freezing data are reported. All temperatures are reported in degrees Celcius. The following abbreviations were used:

P= primary inclusion

S= secondary inclusion

PS= psuedosecondary inclusion

?= questionable whether primary or secondary

2Ø= number of phases present in inclusion

l= liquid phase present

v= vapor phase present

APPENDIX II

Fluid Inclusion Data

Central Tennessee Mining District

Sample Number: Cu-15 1231 Host Mineral: Sphalerite

Inclusion Type	Homogenization Temperature	Freezing Temperature
P 2Ø 1-v	104.4	-17.9
P 2Ø 1-v	105.0	-17.7
P 2Ø 1-v	127.1	
P 2Ø 1-v	100.2	
P 2Ø 1-v	103.7	
P 2Ø 1-v	99.6	
S 2Ø 1-v	75.1	
S 2Ø 1-v	77.8	

Sample Number: Cu-24 1143-1145 Host Mineral: Sphalerite

Inclusion Type	Homogenization Temperature	Freezing Temperature
P 2Ø 1-v	108.2	
P 2Ø 1-v	111.0	
P 2Ø 1-v	111.7	
P 2Ø 1-v	100.0	
P 2Ø 1-v	116.3	
P 2Ø 1-v	139.0	
P 2Ø 1-v	119.1	
P 2Ø 1-v	101.1	
P 2Ø 1-v	121.1	
P 2Ø 1-v	121.2	-21.6
P 2Ø 1-v	124.9	-21.3
P 2Ø 1-v	126.9	-21.0
? 2Ø 1-v		-22.7
? 2Ø 1-v		-23.2
? 2Ø 1-v		-20.9
S 2Ø 1-v	82.9	
S 2Ø 1-v	70.6	
S 2Ø 1-v	88.0	

Sample Number: Cu-35 1109-1111 Host Mineral: Sphalerite

Inclusion Type	Homogenization Temperature	Freezing Temperature
P 2Ø 1-v	124.9	
P 2Ø 1-v	122.0	
P 2Ø 1-v	112.9	
P 2Ø 1-v	125.9	

P 2∅ 1-v	116.9	
P 2∅ 1-v	96.7	
P 2∅ 1-v	88.5	
P 2∅ 1-v	93.1	
P 2∅ 1-v	100.4	
P 2∅ 1-v	109.6	
P 2∅ 1-v	119.6	
P 2∅ 1-v	106.7	-20.1
P 2∅ 1-v	108.9	-17.9
PS 3∅ 1-1-v	115.4	-19.7
PS 3∅ 1-1-v	110.8	

Sample Number: Cz-74 1045 Host Mineral: Sphalerite

Inclusion Type	Homogenization Temperature	Freezing Temperature
P 2∅ 1-v	100.4	
P 2∅ 1-v	99.6	
P 2∅ 1-v	95.3	
P 2∅ 1-v	99.3	-21.6
P 2∅ 1-v	101.8	
P 2∅ 1-v	100.4	
P 2∅ 1-v	101.7	
P 2∅ 1-v	98.4	
P 2∅ 1-v	102.4	
P 2∅ 1-v	85.4	
P 2∅ 1-v	87.6	
P 2∅ 1-v	80.3	
P 2∅ 1-v	83.8	

Sample Number: P-5 810-811 Host Mineral: Fluorite

Inclusion Type	Homogenization Temperature	Freezing Temperature
P 2∅ 1-v	108.1	-18.1
P 2∅ 1-v	108.5	-18.2
P 2∅ 1-v	114.6	
P 2∅ 1-v	109.3	-15.4
P 2∅ 1-v	137.5	
P 2∅ 1-v	90.3	-12.9
P 2∅ 1-v	95.7	
P 2∅ 1-v	102.1	
P 2∅ 1-v	103.9	
P 2∅ 1-v	103.0	
P 2∅ 1-v	104.2	
P 2∅ 1-v	114.4	
P 2∅ 1-v	107.8	
P 2∅ 1-v	103.9	
P 2∅ 1-v	103.5	
P 2∅ 1-v	102.9	
P 2∅ 1-v	104.7	

Sample Number: P-5 1160 Host Mineral: Fluorite

Inclusion Type	Homogenization Temperature	Freezing Temperature
P 2Ø 1-v	128.8	-14.3
P 2Ø 1-v	122.4	-14.4
P 2Ø 1-v	126.9	-15.2
P 2Ø 1-v	124.0	
P 2Ø 1-v	116.2	
P 2Ø 1-v	112.8	
P 2Ø 1-v	113.2	
P 2Ø 1-v	106.9	
P 2Ø 1-v	120.3	
P 2Ø 1-v	105.4	
P 2Ø 1-v	127.6	
P 2Ø 1-v	123.5	
P 2Ø 1-v	123.6	
S 2Ø 1-v	78.4	-15.0

Hansonburg Mining District

Sample Number: MT-1A Host Mineral: Quartz

Inclusion Type	Homogenization Temperature	Freezing Temperature
P 2Ø 1-v	186.2	
P 2Ø 1-v	159.2	
P 2Ø 1-v	180.5	
P 2Ø 1-v	185.5	
P 2Ø 1-v	197.0	
P 2Ø 1-v	220.0	
P 2Ø 1-v	148.7	
P 2Ø 1-v	163.0	
P 2Ø 1-v	174.5	
P 2Ø 1-v	142.2	
P 2Ø 1-v	179.1	
P 2Ø 1-v	202.0	
P 2Ø 1-v	180.7	
P 2Ø 1-v	221.0	
P 2Ø 1-v	197.1	

Sample Number: HH-1 Host Mineral: Calcite

Inclusion Type	Homogenization Temperature	Freezing Temperature
P 2Ø 1-v	98.8	
P 2Ø 1-v	102.7	
P 2Ø 1-v	120.2	
P 2Ø 1-v	108.2	
P 2Ø 1-v	112.3	
P 2Ø 1-v	111.7	

P 2Ø 1-v	102.1
P 2Ø 1-v	107.6
P 2Ø 1-v	107.2
P 2Ø 1-v	113.3
P 2Ø 1-v	101.1
P 2Ø 1-v	99.6
P 2Ø 1-v	113.6
P 2Ø 1-v	105.6

Continental Mine

Sample Number: MP-2

Host Mineral: Calcite

Inclusion Type	Homogenization Temperature	Freezing Temperature
P 2Ø 1-v	291	
P 2Ø 1-v	286	
P 2Ø 1-v	263	
P 2Ø 1-v	248	
P 2Ø 1-v	292	
P 2Ø 1-v	267	
P 2Ø 1-v	305	
P 2Ø 1-v	255	
P 2Ø 1-v	259	
P 2Ø 1-v	280	
P 2Ø 1-v	228	
P 2Ø 1-v	202	
S 2Ø 1-v	160.4	

Sample Number: MP-3

Host Mineral: Marble

Inclusion Type	Homogenization Temperature	Freezing Temperature
P 2Ø 1-v	270	
P 2Ø 1-v	291	
P 2Ø 1-v	315	
P 2Ø 1-v	300	
P 2Ø 1-v	250	
P 2Ø 1-v	202	
P 2Ø 1-v	330	
P 2Ø 1-v	290	

Sample Number: MLV-8

Host Mineral: Marble

Inclusion Type	Homogenization Temperature	Freezing Temperature
P 2Ø 1-v	341	
P 2Ø 1-v	321	
P 2Ø 1-v	332	
P 2Ø 1-v	312	

P 2Ø	1-v	347
P 2Ø	1-v	327
P 2Ø	1-v	336
P 2Ø	1-v	329
P 2Ø	1-v	300
P 2Ø	1-v	320
P 2Ø	1-v	332
P 2Ø	1-v	351
P 2Ø	1-v	337

APPENDIX III

Silica Crystallite Size Data

Central Tennessee Mining District

Sample Number	Silica Crystallite Size (Å)	Temperature (°C)
Cu-15 1230	1109	263
Cu-15 1232	1065	259
Cu-34 1446-1449 (D)	623	212
Cu-34 1446-1449 (D)	839	236
Cu-34 1446-1449 (L)	858	237
Cu-34 1446-1449 (L)	665	217
Cu-34 1466 (L)	986	251
Cu-34 1466 (L)	1086	261
Cu-34 1466 (D)	859	239
Cu-34 1466 (D)	968	250
Cu-35 759 (L)	819	235
Cu-35 759 (L)	838	237
Cu-35 759 (D)	471	190
Cu-35 759 (D)	641	214
Cu-35 1117	766	229
Cz-38 901	719	223
Cz-38 1201	895	242

Hansonburg Mining District

MT-1A	705	222
MT-9 (L)	755	228
MT-9 (L)	641	214
MT-9 (D)	612	210
MT-9 (D)	560	203
MT-10	674	218
MT-11	710	222
MT-26	687	220
HH-1 (L)	645	215
HH-1 (L)	608	210
HH-1 (D)	546	201
HH-1 (D)		214

Continental Mine

MP-3	106,468	2907
------	---------	------

Note: D=Dark Fraction; L=Light Fraction

This thesis is accepted on behalf of the faculty
of the Institute by the following committee:

David J. Womack

Advisor

[Signature]

David B. John

Archie Campbell

Nov. 3rd 1975

Date